# Elevated Cyclin G2 Expression Intersects with DNA Damage Checkpoint Signaling and Is Required for a Potent $G_2/M$ Checkpoint Arrest Response to Doxorubicin*[S]

**Maike Zimmermann**[‡§], **Aruni S. Arachchige-Don**[§1], **Michaela S. Donaldson**[‡], **Robert F. Dallapiazza**[§2], **Colleen E. Cowan**[§3], and **Mary C. Horne**[‡§4]

*From the ‡Department of Pharmacology, University of California, Davis, California 95616 and the §Department of Pharmacology, University of Iowa, Iowa City, Iowa 52242*

**Background:** DNA damage triggers cell cycle checkpoints to halt cell division ahead of DNA repair.
**Results:** Ectopic cyclin G2 (CycG2) induces a Chk2-dependent cell cycle arrest, and depletion of endogenous CycG2 attenuates doxorubicin-induced $G_2/M$-phase cell cycle arrest.
**Conclusion:** CycG2 influences checkpoint signaling and is required for $G_2/M$ arrest responses to genotoxic stress.
**Significance:** Proper checkpoint function is important for genomic integrity and tumor suppression.

To maintain genomic integrity DNA damage response (DDR), signaling pathways have evolved that restrict cellular replication and allow time for DNA repair. *CCNG2* encodes an unconventional cyclin homolog, cyclin G2 (CycG2), linked to growth inhibition. Its expression is repressed by mitogens but up-regulated during cell cycle arrest responses to anti-proliferative signals. Here we investigate the potential link between elevated CycG2 expression and DDR signaling pathways. Expanding our previous finding that CycG2 overexpression induces a p53-dependent $G_1/S$ phase cell cycle arrest in HCT116 cells, we now demonstrate that this arrest response also requires the DDR checkpoint protein kinase Chk2. In accord with this finding we establish that ectopic CycG2 expression increases phosphorylation of Chk2 on threonine 68. We show that DNA double strand break-inducing chemotherapeutics stimulate CycG2 expression and correlate its up-regulation with checkpoint-induced cell cycle arrest and phospho-modification of proteins in the ataxia telangiectasia mutated (ATM) and ATM and Rad3-related (ATR) signaling pathways. Using pharmacological inhibitors and ATM-deficient cell lines, we delineate the DDR kinase pathway promoting CycG2 up-regulation in response to doxorubicin. Importantly, RNAi-mediated blunting of CycG2 attenuates doxorubicin-induced cell cycle checkpoint responses in multiple cell lines. Employing stable clones, we test the effect that CycG2 depletion has on DDR proteins and signals that enforce cell cycle checkpoint arrest. Our results suggest that CycG2 contributes to DNA damage-induced $G_2/M$ checkpoint by enforcing checkpoint inhibition of CycB1-Cdc2 complexes.

Genomic DNA is continually subject to lesions induced by environmental radiation, chemical carcinogens, and reactive oxygen species generated by cellular metabolism (1). If damage to chromosomal DNA is not corrected, these insults will lead to genomic instability and cancer. The presence of a lesion is relayed within minutes of the genomic insult through DNA damage response (DDR)[5] signal-transduction pathways. Signaling cascades including sensor, transducer, and effector proteins carry out a particular response (*e.g.* induction of cell-cycle arrest, DNA repair or apoptosis) dependent on the type and extent of the damage. Damage sensors initiate distinct DDR signaling pathways to coordinate activation of one of the phosphoinositide 3-kinase-related kinases that plays central roles in maintenance of organismal longevity, ataxia telangiectasia mutated (ATM), ATM and Rad3-related (ATR), and DNA-dependent protein kinase (DNA-PK) (1, 2). ATM kinase activation is primarily stimulated by blunt double-stranded DNA (dsDNA) ends such as the DNA double-strand breaks (DSBs) incurred through γ-irradiation (3), whereas ATR activation is most responsive to single-stranded DNA (ssDNA) like that presented by stalled DNA replication intermediates or resected DSB ends (4). DNA-PK is a critical participant in the non-homologous end-joining pathway for repair of V(D)J recombination-induced DSBs but is also thought to serve a vital DNA repair function during genotoxic stress DDRs (5). However, growing evidence suggests that extensive cross-talk between the DNA damage-responsive phosphoinositide 3-kinase-related kinases exists, the summation of which determines cell fate (4–6).

[S] This article contains supplemental Figs. S1–S10.

[1] Present address: Dept. of Pharmacology, Cancer Institute of New Jersey, UMDNJ-Robert Wood Johnson Medical School, Research Tower, Rm. 561, 675 Hoes Lane, Piscataway, NJ 08854.
[2] Present address: Dept. of Neurological Surgery, University of Virginia, Charlottesville, VA 900812.
[3] Present address: Rush University Medical Center, Chicago, Il 60612.
[4] To whom correspondence should be addressed: Dept. of Pharmacology, Tupper Hall, Rm. 2219B, 451 E. Health Sciences Drive, University of California, Davis, CA 95616-8636. Tel.: 530-752-7723; Fax: 530-752-7710; E-mail: mhorne@ucdavis.edu.

[5] The abbreviations used are: DDR, DNA damage response; ATM, ataxia telangiectasia mutated; ATR, ATM and Rad3-related; DNA-PK, DNA-dependent protein kinase; DSB, double strand break; KD, knock-down; ANOVA, analysis of variance; NSC, non-silencing control shRNA; CycB1, cyclin B1; RFP, red fluorescent protein; PP2A, protein phosphatase 2A; Dox, doxorubicin.

DNA DSBs pose the most significant problem for maintenance of genomic stability. ATM is critical for the initial response to DSBs (3). The Mre11-Rad50-Nbs1 sensor complex (MRN (Mre11-Rad50-Nbs1) complex) promotes ATM activation and recognition of DSBs (3). It facilitates trans-autophosphorylation of inactive ATM dimers on Ser-1981 and thereby ATM dissociation into catalytically active monomers (3). Activated ATM interacts with and phosphorylates numerous proteins to amplify and propagate the signal. Studies indicate ATR is also activated by DSBs and plays a role in the later phase of the response, the progressive resection of blunt end DSB junctions to single strand ends ultimately triggering ATR activation (4, 7). Once activated, ATM and ATR phospho-activate their respective target checkpoint kinases, Chk2 and Chk1. Chk1 and Chk2 in turn phosphorylate and modulate the activity of downstream effectors (Cdc25s A, B, and C; p53) to ultimately halt progression of cells through $G_1$- and $G_2$-phase checkpoints (3, 4, 6, 8). This blockade of cellular proliferation allows DNA repair to proceed, but if the DNA damage is irreparable, cell death via apoptosis will ensue.

*CCNG2* encodes cyclin G2 (CycG2), an unconventional cyclin homolog linked to cell cycle inhibition (9–17). *CCNG2* mRNAs are moderately expressed in proliferating cells (peaking during the late S/early $G_2$ phase) (9, 11, 12) but significantly up-regulated as cells exit the cell cycle in response to receptor-mediated negative signaling in B-lymphocytes and ovarian cancer cells (12, 17). Transcript data from a variety of studies indicate that *CCNG2* expression is up-regulated during cell cycle arrest responses to diverse growth-inhibitory signals and strongly repressed by mitogens, suggesting a positive role for CycG2 in the promotion or maintenance of cell cycle arrest (12, 18–24). *CCNG2* transcripts are also increased in cells treated with the DNA damaging chemotherapeutics actinomycin D and ecteinascidin-743 (25, 26). In contrast to *CCNG1* (the gene encoding the CycG2 homolog CycG1 (27, 28)), *CCNG2* does not contain p53 binding sites (29), but recent work showed that *CCNG2* is a transcriptional target of the p53 homolog, p63 (30). Importantly, suppressed *CCNG2* mRNA expression has been linked to cancer, including thyroid, oral, and breast carcinomas (14, 30, 31).

In previous work we determined that ectopic CycG2 expression inhibits DNA synthesis and induces a $G_1$/S-phase arrest in a variety of cell lines (13, 15, 16). We showed that overexpression of CycG2 inhibits CDK2 activity and that the CycG2-mediated $G_1$/S-phase cell cycle arrest is p53-dependent (13, 15). Subsequent studies determined that even moderate up-regulation of ectopic CycG2 expression inhibits cellular proliferation (10, 16, 24). We found that exogenous and endogenously expressed CycG2 is a CRM1-dependent nucleocytoplasmic shuttling protein that localizes to the cytoplasmic-cytoskeletal compartment of replicating cells where it associates with centrosomes via AKAP450 (15). Here we examine CycG2 expression during cellular responses to treatment with the chemotherapeutic DNA DSB-inducing topoisomerase II poisons (32), etoposide, and doxorubicin. We relate changes in CycG2 expression to the effects doxorubicin treatment has on cell cycle progression and induction of phospho-activated forms of ATM/ATR pathway DDR proteins. By using transient overexpression of recombinant CycG2 and shRNA-mediated RNAi to knockdown endogenous CycG2, we investigate the involvement of CycG2 with DDR signaling pathways and its contribution to DNA damage-induced cell cycle arrest.

## EXPERIMENTAL PROCEDURES

*Cell Culture and Treatment*—U2OS, HCT116 parental, p53$^{-/-}$, p21$^{-/-}$, and Chk2$^{-/-}$ (kind Gift of Dr. B. Vogelstein) were cultured in high glucose DMEM (Invitrogen) supplemented with 10% heat-inactivated fetal bovine serum (Atlanta Biologicals), 100 units/ml penicillin, 100 $\mu$g/ml streptomycin sulfate (Invitrogen), and 1 mM sodium pyruvate (Sigma). NIH3T3 cells were grown in DMEM supplemented with 10% heat-inactivated calf serum (Cellgro), 100 units/ml penicillin, and 100 $\mu$g/ml streptomycin sulfate. MCF7 cells were cultured in minimum essential medium with Earle's salts (Invitrogen) supplemented with 10% heat-inactivated FBS, 2 mM L-glutamine (Research Products International, IL), 1 mM sodium pyruvate, 100 units/ml penicillin, 100 $\mu$g/ml streptomycin sulfate, and 10 $\mu$g/ml bovine insulin (Sigma). MCF10a cells were cultured in DMEM/Ham's F-12 (1:1) (Invitrogen) supplemented with 5% heat-inactivated horse serum (Cellgro), 100 ng/ml cholera toxin (Calbiochem), 20 ng/ml EGF (Invitrogen), 10 $\mu$g/ml insulin, 500 ng/ml hydrocortisone (Sigma), 2 mM L-glutamine, 100 units/ml penicillin, and 100 $\mu$g/ml streptomycin. SV40-transformed normal (GM00637) and ATM-deficient (GM05849) human fibroblast cells were purchased from Coriell Cell Repositories (Camden, NJ) and cultured in minimum essential medium with Earle's salts, 10–15% heat-inactivated FBS, 2 mM L-glutamine, with a 2× concentration of essential and nonessential amino acids and vitamins. All cultures were plated at 20–30% and maintained at 50–90% confluency in a humidified chamber at 37 °C with 5% $CO_2$. DNA damage was induced in the specified cultures by treatment with the chemotherapeutic agents (Sigma) doxorubicin hydrochloride (345 nM) or etoposide (30 $\mu$M) for the indicated time periods. Where indicated, cultures were preincubated with 3 mM caffeine (Sigma) or 10 $\mu$M KU55933 (Calbiochem) for 1 h before the addition of doxorubicin.

*shRNA Expression Constructs and Establishment of Stable Clones*—DNA constructs for expression of V5- and GFP-epitope tagged CycG2 fusion proteins in mammalian cells have been described (13, 15). Selection of shRNA target sites was done following the guidelines provided on Ambion "siRNA Target Finder and Design Tool." Efficacy and specificity of all CycG2-targeting and nonsilencing controls was verified via cotransfection assays (see supplemental Fig. S2). Generation of pSilencer-RFP constructs harboring targeting and control shRNAs was as follows. The CMV promoter-driven RFP-coding cassette was PCR-amplified from pDsRed2-C1 and subcloned into KpnI-linearized pSilencer 1.0-U6 (Ambion; Austin, TX). For each shRNA construct, the shRNA insert was prepared by PCR annealing forward and reverse oligonucleotides and ligating into the pSilencer-RFP vector that had been sequentially digested with ApaI and EcoRI. To the reverse oligonucleotide sequence, ApaI and EcoRI restriction endonuclease sites were engineered. The oligonucleotides were ordered from Integrated DNA Technologies (Coralville, IA). The oligonucleotide sequences are as follows (the stem-loop sequence is shown in

capital letters, and the restriction site is shown in lowercase): Ex4.2 forward (5′-GCTACCACTGCCTTAAACTTTCAAG-AGAAGTTTAAGGCAGTGGTAGCTTTTT-3′) and reverse (5′-aattAAAAAGCTACCACTGCCTTAAACTTCTCTT-GAAAGTTTAAGGCAGTGGTAGCggcc-3′); NSC forward (5′-GCTCCCACCACCTTAAACTTTCAAGAGAAGTTTA-AGGTGGTGGGAGCTTTTT-3′) and reverse (5′-aattAAA-AAGCTCCCACCACCTTAAACTTCTCTTGAAAGTTTA-AGGTGGTGGGAGCggcc-3′); sh 1-B forward (5′-GCTAC-TACTGCCTTAAACTTTCAAGAGAAGTTTAAGGCAGT-AGTAGCTTTTT-3′) and reverse (5′-aattAAAAAGCTACT-ACTGCCTTAAACTTCTCTTGAAAGTTTAAGGCAGTA-GTAGCggcc-3′). All constructs were verified by DNA sequencing. The pGeneClip hMGFP ID3 shRNA (stem-loop, CCCGGAGAATGATAACACTTTCTTCCTGTCAAAAGT-GTTATCATTCTCCGGG) designed against a different target site and non-targeting NC control shRNA (stem-loop, GGAA-TCTCATTCGATGCATACCTTCCTGTCAGTATGCATC-GAATGAGATTCC) were purchased from SABiosciences (Frederick, MD).

For production of clonal population of cells stably expressing shRNAs, the vector pSuper.retro.puro (Oligoengine; Seattle, WA) encoding a puromycin resistance gene was used. The oligonucleotides annealed and subcloned into BglII/HindIII-digested pSuper.retro.puro were as follows (the stem-loop sequence is in capital letters, and the restriction site is in lowercase): sh ID3 forward (5′-gatcCCCGGAGAATGATAA-CACTTTCTTCCTGTCAAAAGTGTTATCATTCTCCGG-GTTTTT-3′) and reverse (5′-agctAAAAACCCGGAGAATG-ATAACACTTTTGACAGGAAGAAAGTGTTATCATTCT-CCGGG-3′); sh 1-B forward (5′-gatcGCTACTACTGCCTTA-AACTTTCAAGAGAAGTTTAAGGCAGTAGTAGCTT-TTT-3′) and reverse (5′-agctAAAAAGCTACTACTGCCTT-AAACTTCTCTTGAAAGTTTAAGGCAGTAGTAGC-3′); NSC forward (5′gatcGCTCCCACCACCTTAAACTTTCAA-GAGAAGTTTAAGGTGGTGGGAGCTTTTT-3′) and re-verse (5′-agctAAAAAGCTCCCACCACCTTAAACTTCTC-TTGAAAGTTTAAGGTGGTGGGAGC-3′). For selection of stable MCF7 clones, freshly established cultures were trans-fected with NdeI-linearized vector using Lipofectamine 2000 (Invitrogen). One day later cells were reseeded at different den-sities onto new dishes and plates. The following day selection for puromycin-resistant clones was started by an exchange of culture medium containing 3 μg/ml puromycin. Selected clonal populations were expanded and tested for their ability to suppress expression of exogenous and endogenous human CycG2 by immunoblot analysis (see supplemental Fig. S8).

*Antibodies (Source and Dilutions)*—Anti-α-tubulin (DM1A, MS-581, 1:10,000), anti-Chk2 (MS-1515, 1:2000), and anti-p53 (MS-186, 1:1000) mouse monoclonal antibodies were obtained from NeoMarkers. Mouse anti-GAPDH (MAB374, 1:200 000) was obtained from Millipore. Rabbit anti-phospho-Chk2-(Thr-68) (#2661, 1:500), anti-phospho-Chk1(Ser-345) and -pChk1(Ser-296) (#2341 and #2349, each 1:500), anti-Chk1 (#2360, 1:4000), anti-phospho-ATM(Ser-1981) (#4526, 1:500), anti-ATM (#2873, 1:500), anti-phospho-SMC1(Ser-957) (#4805, 1:1000), anti-phospho-Cdc2(Tyr-15) (#9111, 1:1000), anti-cyclin B1 (#4138, 1:100), anti-Nbs1 (#3002, 1:500), and

anti-β-actin (#4970, 1:4000) antibodies were purchased from Cell Signaling. Mouse anti-phospho-Nbs1(Ser-343) (NB100−92610, 1:500) antibodies were obtained from Novus Biologicals. The C-18 rabbit anti-CycG1 (sc-320, 1:150) and goat anti-lamin B (sc-6217, 1:80) and mouse anti-Cdc2 (sc-54, 1:1000) antibod-ies were purchased from Santa Cruz Biotechnology. Sheep anti-α-tubulin (ATN02, 1:100) and mouse anti-γ-tubulin (GTU-88, T6557, 1:400) were purchased from Cytoskeleton (Denver, CO) and Sigma, respectively. HRP-conjugated secondary antibodies against rabbit and mouse IgG (1:5000) were purchased from Bio-Rad and Jackson ImmunoResearch. Alexa 488-, 568-, and 660-conjugated secondary antibodies (1:1000) were purchased from Molecular Probes/Invitrogen. The CycG2-specific anti-bodies 68232 (1:300) and 68964 (1:500) produced in our labo-ratory were affinity-purified from rabbit anti-sera and tested for specificity toward CycG2 fusion proteins (see supplemental Fig. S1) essentially as described (13, 15). The rabbit anti-CycG1 antibody 1133 (1:150) was generated against the peptide KLL-HQLNALEQES corresponding to amino acids 12–24 of human CycG1, affinity-purified on resin-bound CycG1GST fusion proteins, and tested for sensitivity and specificity (see supple-mental Fig. S1) as described (13, 33).

*Immunoblot Analysis*—Cells were lysed in radioimmune pre-cipitation assay buffer (10% glycerol, 1% Nonidet P-40, 0.4% deoxycholate, 0.05% SDS, 150 mM NaCl, 10 mM EDTA, 5 mM EGTA, 50 mM Tris, pH 7.4) containing protease inhibitors (pepstatin A (1 μg/ml), leupeptin (1 μg/ml), aprotinin (2 μg/ml), and phenylmethanesulfonyl fluoride (200 nM)) and phosphatase inhibitors (sodium fluoride (25 mM), sodium pyro-phosphate (25 mM), *p*-nitrophenyl phosphate (1 mM), and microcystin (2 μM)). Cell lysates were centrifuged at $10,000 \times g$ to remove insoluble material. Protein concentration was meas-ured using BCA reagent (Pierce). Protein lysates were fraction-ated by SDS-PAGE, blotted onto PVDF membranes, and sub-jected to immunoblotting as previously described (13, 15).

*Immunofluorescence Microscopy*—MCF10a cells were seeded at $1.5 \times 10^5$ cells/35-mm well onto a 22-mm-square glass coverslip coated with 10 mg/ml collagen and 1 μg/ml poly-L-lysine (Sigma) 14–18 h before treatment. Coverslips were removed 16 h after treatment, rinsed with PBS, and imme-diately fixed with ice-cold MeOH at −20 °C for 5 min. Speci-mens were stained and mounted, and images were collected by confocal microscopy as described (13).

*Cell Cycle Analysis by Flow Cytometry*—DNA content in untransfected cell cultures and stable MCF7 clones was assessed after fixation of cells with −20 °C 70% EtOH. Washed pellets of fixed cells were resuspended in PBS containing 0.25 mg/ml RNase A (Fermentas) and 50 μg/ml propidium iodide (Sigma) for 30 min at room temperature before DNA flow cytometry using a FACScan (BD Biosciences) as described (11–13). For cell cycle analysis of propidium iodide-stained DNA in GFP-expressing populations of transiently transfected HCT116, GM05849, and GM00637 cells, the GFP signal was retained by an initial 10-min fixation in PBS containing 0.5% paraformaldehyde and 10 mM EDTA before permeabilization and final fixation with −20 °C 100% methanol as described (13). In some experiments total DNA in live cells transiently express-ing fluorescent marker proteins (*e.g.* GFP or RFP) was stained
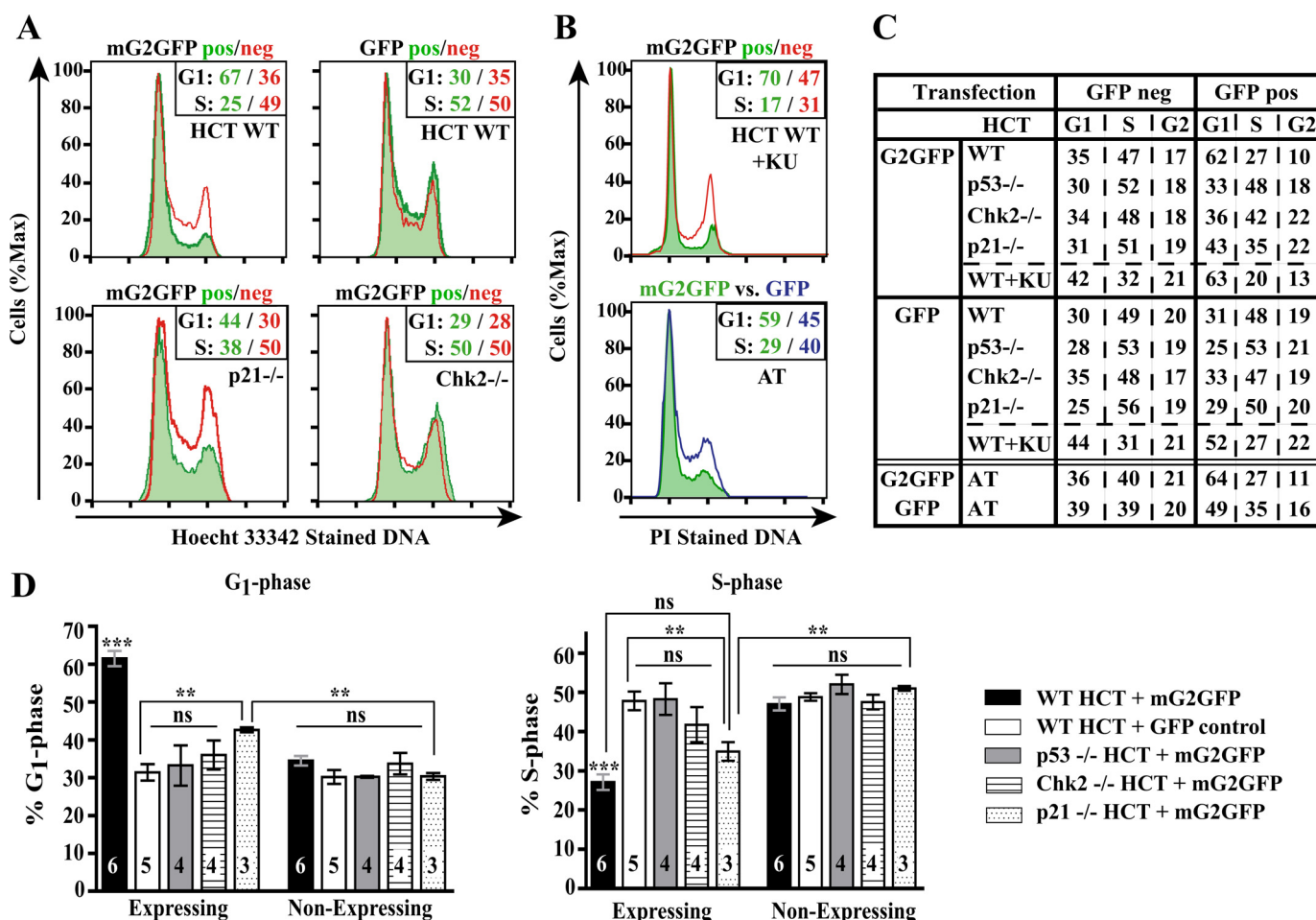
| Transfection | | GFP neg | | | GFP pos | | |
|---|---|---|---|---|---|---|---|
| | HCT | G1 | S | G2 | G1 | S | G2 |
| G2GFP | WT | 35 | 47 | 17 | 62 | 27 | 10 |
| | p53-/- | 30 | 52 | 18 | 33 | 48 | 18 |
| | Chk2-/- | 34 | 48 | 18 | 36 | 42 | 22 |
| | p21-/- | 31 | 51 | 19 | 43 | 35 | 22 |
| | WT+KU | 42 | 32 | 21 | 63 | 20 | 13 |
| GFP | WT | 30 | 49 | 20 | 31 | 48 | 19 |
| | p53-/- | 28 | 53 | 19 | 25 | 53 | 21 |
| | Chk2-/- | 35 | 48 | 17 | 33 | 47 | 19 |
| | p21-/- | 25 | 56 | 19 | 29 | 50 | 20 |
| | WT+KU | 44 | 31 | 21 | 52 | 27 | 22 |
| G2GFP | AT | 36 | 40 | 21 | 64 | 27 | 11 |
| GFP | AT | 39 | 39 | 20 | 49 | 35 | 16 |

FIGURE 1. **Ectopic cyclin G2 expression induces a Chk2-dependent cell cycle arrest but does not require p21 or ATM.** *A,* shown is a representative flow cytometry analysis of DNA content in live parental HCT116 (*WT*) and isogenic $p21^{-/-}$ and $Chk2^{-/-}$ cell cultures transiently transfected with expression plasmids for GFP-tagged CycG2 or control GFP. Histogram overlays of Hoechst 33342 stained DNA in non-expressing (*red line*) and GFP expressing (*green area*) cells from the same transfected culture. *Numbers in the upper right of each histogram panel* indicate the percentage of CycG2GFP- or control GFP-expressing (*left, green type*) and non-expressing (*right, red type*) cell populations in the $G_1$- or S-phases of the cell cycle. *B,* shown is a representative flow cytometry analysis of DNA content in fixed ATM-deficient fibroblasts (*lower panel, AT*) or ATM inhibitor-treated WT HCT116 cells (*upper panel*) transiently transfected with expression plasmids for mCycG2GFP or control GFP. Shown are histogram overlays of propidium iodide (*PI*) stained DNA from KU55933 (*KU*)-treated mCycG2GFP-expressing (*green area*)- or non-expressing (*red line*) WT HCT116 cells in the same culture (*top*) and mCycG2GFP-expressing (*green area*) and GFP-expressing (*blue line*) AT cells *bottom*. The percentage of cells in $G_1$ and S phases is shown in the *upper right of each histogram panel. C,* shown is a summary table of average percentage of population in $G_1$, S, and $G_2$/M phases of GFP expressing and non-expressing populations in the indicated transfected cultures (calculated from a minimum of three experimental repeats). Flow cytometry analysis of cells transfected with the indicated plasmids harvested 30–36 h (HCT116) or 48 h (ATM) post transfection. *D,* shown are a *bar graph* and statistical analysis of $G_1$- and S-phase data presented in *C* using one way ANOVA with Tukey's post hoc test. *Numbers embedded in each bar* represent the number of experimental repeats. ***, $p < 0.001$; **, $p < 0.01$; *ns* indicates no significant difference found between encompassed groups.

with Hoechst 33342, and DNA content in the unfixed fluorescent and non-fluorescent cell populations was assessed via flow cytometry using a quadruple laser LSR II flow cytometer (BD Biosciences) as described (13, 15). In all cases assessment of DNA content distribution and cell cycle analysis was done using FlowJo 8.5 software. For statistical analysis, *t* tests and one-way analysis of variance tests (one-way ANOVA with the Tukey and Bonferroni post hoc tests) were done using Prism 4.0 software (GraphPad Software, Inc.). For indicated experiments, TOPRO negative cells were sorted on the basis of GFP expression with a MoFlo cell sorter (Beckman Coulter).

## RESULTS

*Cyclin G2-induced Cell Cycle Arrest Requires p53 and Chk2 but Is Only Partially p21-dependent*—We reported that CycG2 induces a p53-dependent cell cycle arrest in HCT116 cells (15).

Here we examined the effect of ectopic GFP-tagged CycG2 *versus* GFP expression on cell cycle progression in HCT116 cells nullizygous for the DNA damage checkpoint protein Chk2 and compared the effects to those observed in similarly transfected p53 null, p21 null, and wild-type (WT) cells. As anticipated, ectopic expression of GFP alone had no discernable effect on cell cycle progression in any of the isogenic cell lines, the cell cycle profile of each transfected population being similar to the non-expressing controls (Fig. 1, *A* and *C*). Multiple experimental repeats indicated that the $G_1$/S-phase cell cycle arrest induced by ectopic CycG2 expression requires both the presence of Chk2 and p53 (*p* values <0.001), whereas loss of the p53 target gene p21 had only a moderate effect on CycG2 inhibitory activity (Fig. 1, *C* and *D*). As Chk2/p53 checkpoint signaling is triggered by DNA damage-activated ATM, we tested whether ATM is required for the $G_1$/S-phase cell cycle arrest induced by
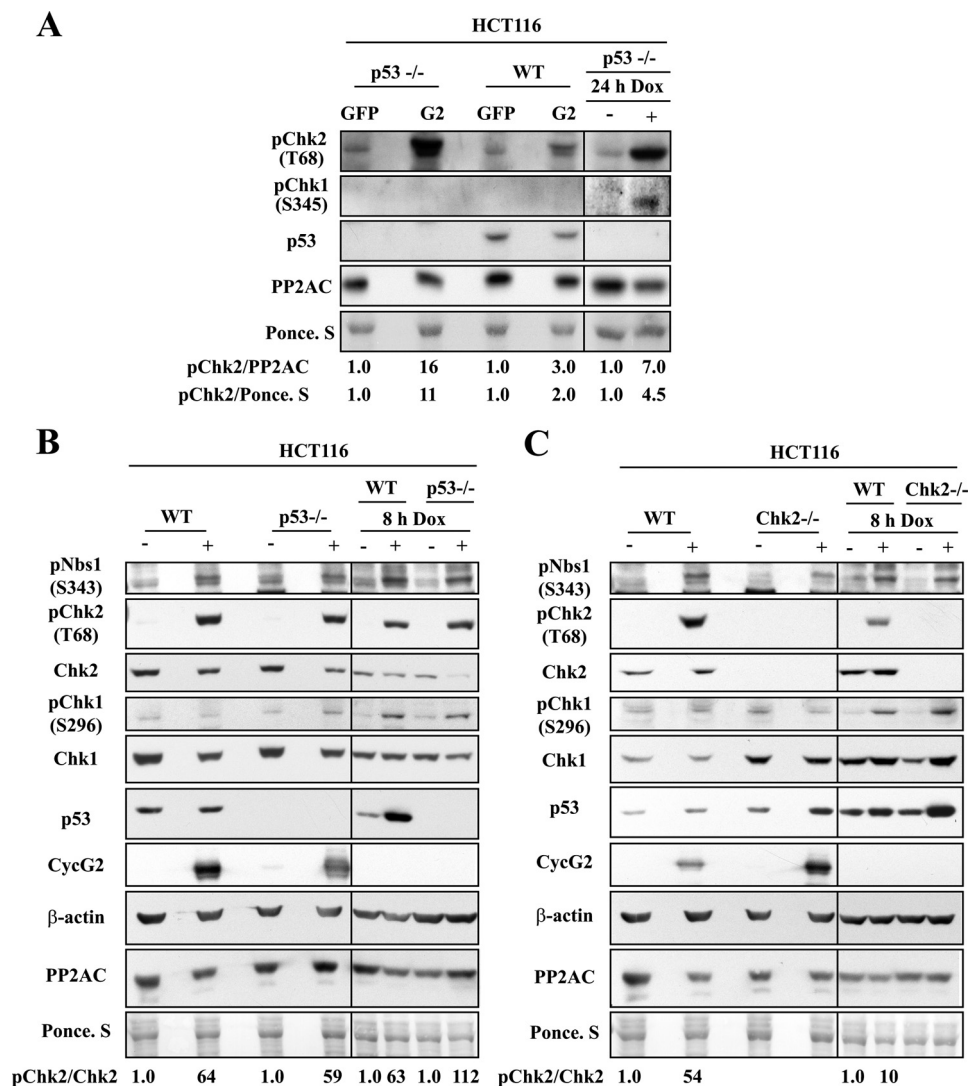
FIGURE 2. **Ectopic expression of CycG2 induces expression of phospho-activated forms of Chk2 and Nbs1 but not Chk1.** *A–C*, shown are immunoblots of proteins in total lysates isolated from transiently transfected cultures of the specified cell lines probed with antibodies directed against the indicated proteins. *A*, expression of pChk2(Thr-68), pChk1(Ser-345), and p53 compared with total PP2A/C in transfected WT and p53$^{-/-}$ HCT116 cells is shown. Control immunoblots for checkpoint proteins in cell lysates from cultures treated for 24 h with (+) doxorubicin (*Dox*) or vehicle (−) are shown at the *right*. Protein loading was assessed by PP2A/C immunoblot, and total protein bands were labeled with Ponceau S (*Ponce. S, bottom panel*). *B* and *C*, expression levels of pNBS1(Ser-343), pChk2 (Thr-68), pChk1(Ser-296), and p53 were compared with total Chk2, Chk1, CycG2, PP2A/C, and β-actin in transiently transfected GFP-sorted WT and p53$^{-/-}$ (*B*) or WT and Chk2$^{-/-}$ (*C*) HCT116 cells. Expression levels in cells treated for 8 h with Dox served as positive controls. Protein loading was assessed by PP2A/C immunoblot and total protein bands were labeled with Ponceau S (*bottom panel*). -Fold increase of Chk2 phosphorylation is indicated under the figure.

ectopic CycG2 expression (Fig. 1, *B* and *C*). Incubation of CycG2GFP-transfected cells with 10 $\mu$M of the ATM inhibitor KU55933 (34) did not block the CycG2-induced cell cycle arrest of WT HCT116 cells (Fig. 1, *B* and *C*). Moreover, in contrast to GFP alone, expression of GFP-tagged CycG2 in the ATM null cell line GM05849 triggered a similar decrease in the proportion of cells in S-phase and an increase in those in G$_1$ phase (*p* values <0.01 and 0.001, respectively, Fig. 1, *B* and *C*, and supplemental Fig. S3). Together these results suggest that ectopic CycG2 expression induces a Chk2- and p53-dependent but ATM-independent G$_1$-phase cell cycle arrest.

*Ectopic Cyclin G2 Expression Induces Activation of Checkpoint Kinase Chk2*—We evaluated whether ectopic expression of CycG2 modulates Chk2 and other DDR signaling proteins. HCT116 wild-type and isogenic p53-null cells were transfected with either GFP or CycG2GFP expression vectors and assessed

for expression of phospho-activated Chk2 and Chk1 (Fig. 2*A*). HCT116 cells treated with doxorubicin served as positive controls for induction of pChk1(Ser-345) and pChk2(Thr-68). We found in reproducible experiments that pChk2(Thr-68) expression was elevated in CycG2GFP compared with GFP-transfected cell lysates (Fig. 2*A*). Interestingly, pChk2(Thr-68) levels were most prominent in the p53 null cultures expressing CycG2GFP. In contrast to the pChk1(Ser-345) levels in doxorubicin treated cells, pChk1(Ser-345) expression was undetectable in transfected p53 null and WT HCT116 cell lysates. As p53 activation is downstream of Chk2 and promotes both cell cycle arrest and cell death, this finding suggests that CycG2GFP expression and the concomitant induction of Chk2 activation is better tolerated in p53 null HCT116 cells.

To further investigate this issue and control for differences in transfection efficiency, we repeated the immunoblot analysis
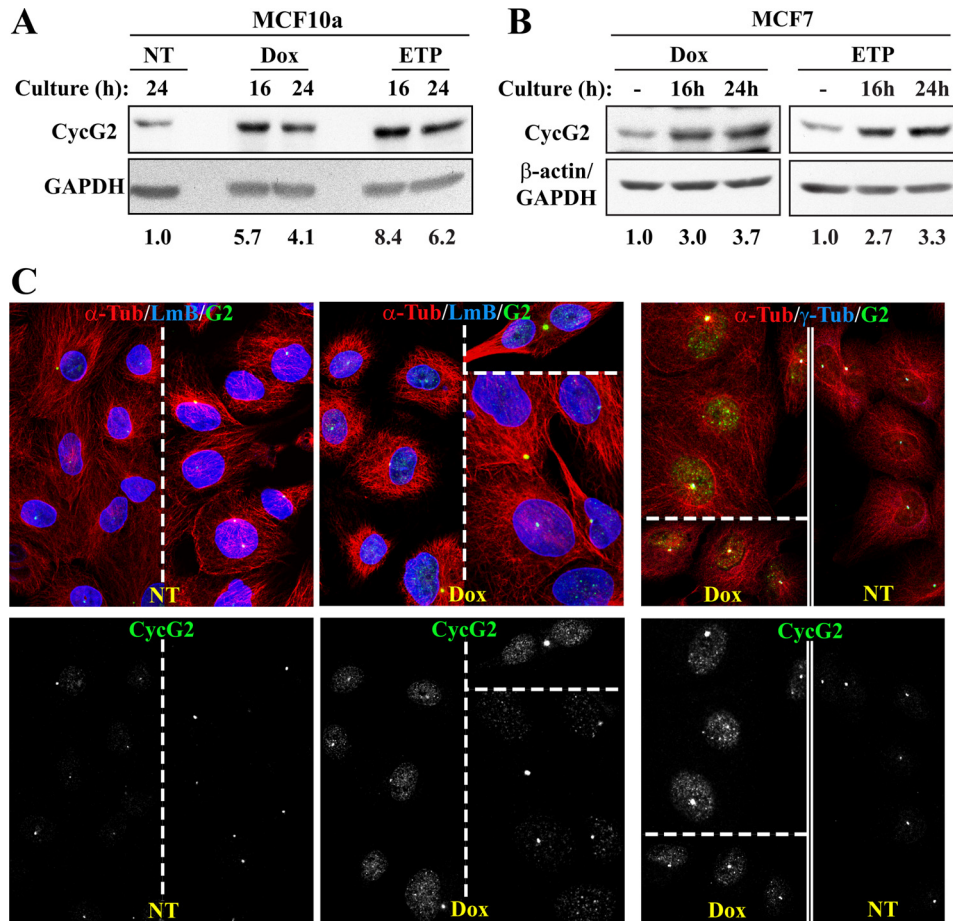
FIGURE 3. **Up-regulated expression and subcellular localization of endogenous CycG2 in cell lines responding to the dsDNA break inducing agents doxorubicin and etoposide.** *A* and *B*, shown are anti-CycG2, GAPDH, and β-actin immunoblots of total protein lysates from doxorubicin (*Dox*), etoposide (*ETP*), or mock-treated (*NT*, −) cultures of MCF10a and MCF7 cells. *A*, shown is quantification of -fold up-regulation of CycG2 expression (*numbers below lanes*) induced by Dox and etoposide treatment relative to loading control (GAPDH) for the indicated time in MCF10a cells. *B*, quantification of CycG2 expression levels induced by Dox and etoposide treatment of MCF7 cells over the indicated time period is shown *below each lane*. *C*, shown is confocal immunofluorescence microscopy optical sections (0.3 μm) of Dox-treated (16 h) and non-treated (*NT*) MCF10a cells. MeOH-fixed cultures were stained with antibodies directed against CycG2 (*G2*, *green*), α-tubulin (*α-Tub*, *red*), and lamin B (*LmB*) or γ-tubulin (γ-*Tub*, *blue*). Shown are multichannel overlay images (pseudo-colored) at the *top*, with corresponding images of the single anti-CycG2 channel (in *black* and *white*) shown directly below. Note basal CycG2 immunosignals in NT cells and increased anti-CycG2 staining at centrosomes and within nuclei of Dox-treated cells.

on FACS-sorted cell populations of similarly transfected WT and p53 null HCT116 cultures (Fig. 2*B*). As before, the non-expressing populations isolated from CycG2GFP-transfected cultures did not show a modulation of phospho-Chk2 or phospho-Chk1 levels. However, lysates isolated from the sorted CycG2GFP-positive populations of both WT and p53 null cultures contained strongly increased levels of pChk2(Thr-68) and moderately elevated pNbs1(Ser-343) expression (Fig. 2*B*). Analogous to results shown in 2*A*, lysates of the CycG2GFP populations did not contain elevated levels of phospho-activated Chk1 (here pChk1(Ser-296); Fig. 2*B*). Repeated sorting experiments showed similar results and verified the specificity of the pChk2(Thr-68) immunosignal (Fig. 2*C* and supplemental Fig. S4). Again, pChk2(Thr-68) and pNbs1(Ser-343) levels were enhanced in CycG2GFP-transfected WT HCT116, but as expected pChk2(Thr-68) was absent in Chk2 null cell lysates (Fig. 2*C*). Moreover, as seen with lysates from unsorted GFP-transfected controls, GFP expression did not modulate pChk2(Thr-68) or pChk1(Ser-345) expression levels (supplemental Fig. S4). Similar results were found for lysates of unsorted U2OS cells transiently transfected with CycG2GFP

expression constructs (supplemental Fig. S4). Together our results show that ectopic up-regulation of CycG2 levels triggers signals that induce expression of phospho-activated forms of Chk2 and Nbs1 but not phospho-Chk1.

*Endogenous Cyclin G2 Is Up-regulated during DNA Damage Responses Induced by Topoisomerase II Inhibitors and Accumulates in Nuclei of Doxorubicin-treated Cells*—Our observations prompted us to investigate CycG2 expression in cells initiating checkpoint signaling in response to chemotherapeutic agent-induced dsDNA breaks. Exposure of the immortalized non-transformed breast epithelial cell line MCF10a to either doxorubicin or etoposide up-regulated CycG2 expression up to 5-fold within the first 4 h of treatment and remained at elevated levels in cultures treated for 24 h (Fig. 3*A*). A comparable response was also observed in similarly treated MCF7 cells (Fig. 3*B*). A similar up-regulation in CycG2 expression (3–5-fold) was observed upon treatment of NIH3T3 and U2OS cells with doxorubicin (supplemental Fig. S5, *A* and *B*).

In unperturbed cells endogenous and exogenous CycG2 behave as centrosome-associated nucleocytoplasmic shuttling proteins (15). We examined the distribution of CycG2 in doxo-
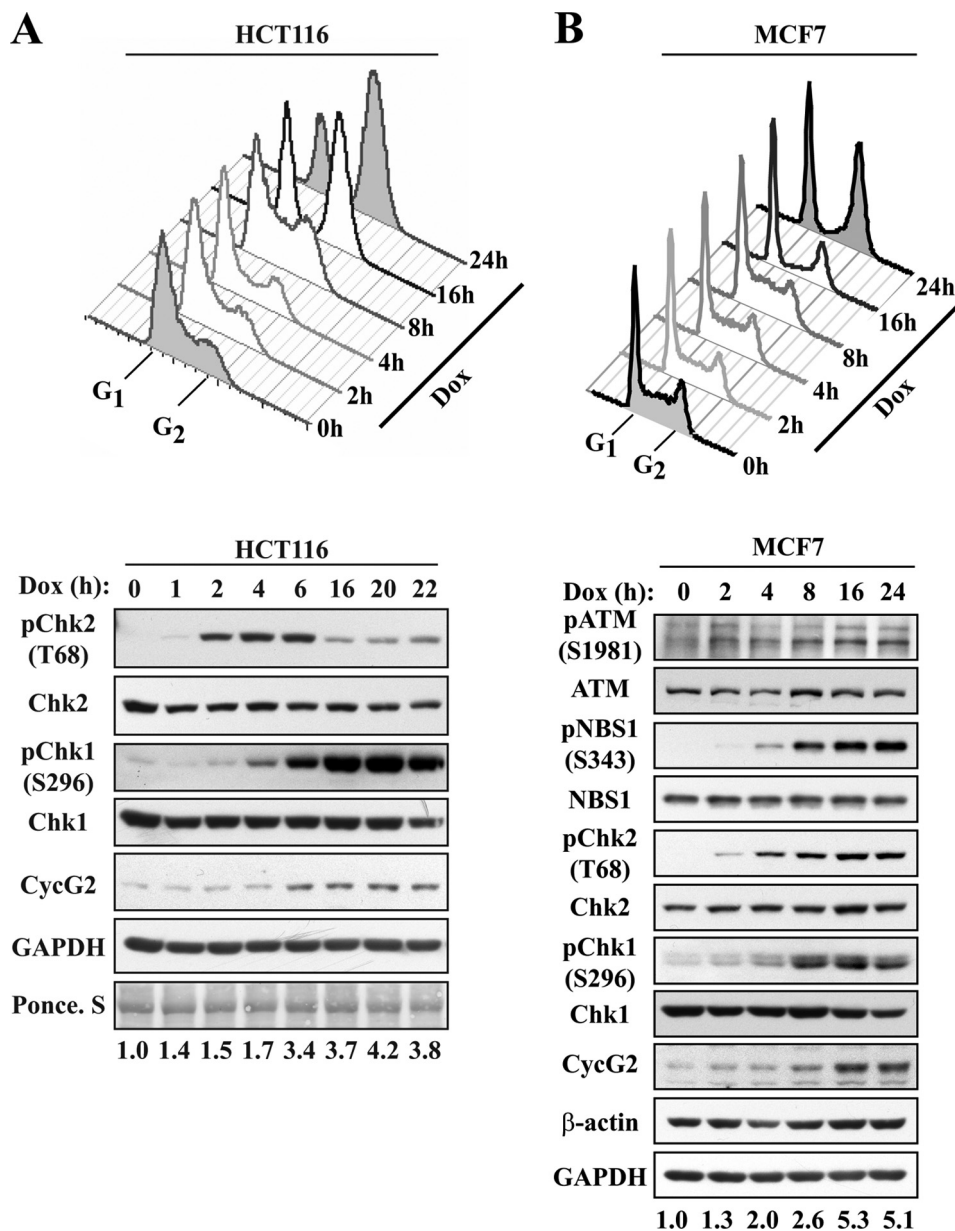
FIGURE 4. **Doxorubicin-induced CycG2 up-regulation follows activation of the ATM signaling pathway but precedes accumulation of cells at the G$_2$-phase checkpoint.** *A* and *B*, *top,* shown are cell cycle profiles of doxorubicin (*Dox*)-treated HCT116 (*A*)and MCF7 (*B*) cultures. *Bottom*, shown is a corresponding immunoblot analysis of proteins induced in HCT116 and MCF7 cultures during the indicated time periods of Dox treatment. CycG2 expression relative to loading controls (*β*-actin, GAPDH, and Ponceau S) is compared with induction of pATM(Ser-1981), pNbs1(Ser-343), pChk2(Thr-68), and pChk1(Ser-296) expression and total protein levels for ATM, Nbs1, Chk2, and Chk1. Densitometry quantification of CycG2 expression relative to loading controls is shown *below each lane.*

rubicin-treated cells. Confocal immunofluorescence microscopy of MCF10a cells showed that doxorubicin-induced up-regulation of CycG2 led to an accumulation of small bright puncta within the nuclei (39% increase in nuclear signal, *p* < 0.0001) of treated cells (Fig. 3*C* and supplement supplemental Fig. S5*C*). Moreover, doxorubicin treatment resulted in a 63% increase in CycG2 abundance at centrosomes (*p* = 0.0018) but as expected did not alter the signal intensity for the integral centrosomal protein γ-tubulin (Fig. 3*C* and supplemental Fig. S5*C*).

To define CycG2 up-regulation in relation to activation of DDR proteins and cell cycle checkpoints, we exposed cultures of murine and human cell lines to 345 nM doxorubicin for up to 24 h, sampling the different cultures over the time course of treatment for immunoblot and cell cycle analysis. HCT116 cells are known to exhibit a minimal S-phase delay in response to DNA DSBs but do undergo a clear and potent DSB-induced G$_1$- and G$_2$-phase checkpoint arrest upon exposure to doxorubicin (Fig. 4*A*). A combination of immunoblot and cell cycle analysis of HCT116 and MCF7 cultures sampled over a time course of treatment determined that the doxorubicin-invoked increase in CycG2 levels trailed phosphorylation of the ATM/ATR target proteins, Chk2 and Chk1, but led the accumulation of cells at the G$_2$/M boundary (Fig. 4, *A* and *B*). Although doxorubicin-induced DNA damage in U2OS and NIH3T3 cells initially results in an apparent delay in S-phase progression, the onset of

a clear $G_2$-phase checkpoint arrest was observed between 8 and 16 h of treatment. CycG2 expression was elevated in NIH3T3 cultures within 4 h of doxorubicin addition, about 2 h after the appearance of phospho-activated forms of ATM and its target SMC1, and remained at increased levels for at least 20 h (supplemental Fig. S6C). A similar analysis of CycG2, pNbs1(Ser-343) and pChk2(Thr-68) expression levels and cell cycle distribution in doxorubicin-treated U2OS cells was performed (supplemental Fig. S6D). Consistently CycG2 up-regulation followed the appearance of phospho-activated forms of early response DDR proteins by about 2 h but preceded the induction of $G_2$-phase checkpoint arrest (Figs. 4 and supplemental Fig. S6).

*Transient Transfection of CCNG2-targeting shRNAs Blunts Doxorubicin-induced $G_2$-phase DNA Damage Checkpoint Arrest Response in NIH3T3 and HCT116 Cells*—To test for the contribution of CycG2 to the doxorubicin-induced cell cycle checkpoint response, we generated and tested *CCNG2*-targeting shRNAs for their ability to knockdown (KD) CycG2 expression levels (supplemental Fig. S2). We transfected cultures with validated shRNA constructs (supplemental Fig. S2) and assayed the effect these shRNAs had on the cell cycle profile of asynchronous cultures grown in the presence or absence of doxorubicin (Fig. 5 and supplemental Fig. S7). NIH3T3 cultures were cotransfected with tracer amounts of GFP expression plasmids and either empty vector (pSilencer) or the pSilencer-Ex4.2 shRNA expression construct. After 48 h of growth, the cultures were treated with doxorubicin for 24 h. Cell cycle analysis of the GFP-expressing populations indicated that cells transfected with the Ex4.2 shRNA plasmid, in contrast to the empty vector control, did not exhibit a potent $G_2$-phase cell cycle arrest response to doxorubicin (supplemental Fig. S7). This suggested a surprising block of the $G_2/M$ rather than the $G_1/S$-checkpoint arrest response by CycG2 knockdown. Repeated experiments in NIH3T3 yielded similar results.

To determine whether the diminished $G_2/M$ checkpoint response in cells expressing CycG2-targeting shRNA is reproducible in human cell lines, analogous experiments with HCT116 cells were performed. HCT116 cultures were transfected with control (NSC or empty vector) or *CCNG2*-targeting (sh 1-B, ID3) shRNA vectors containing expression cassettes for marker fluorescent protein (RFP or GFP) and incubated for 72 h before the addition of doxorubicin or vehicle. After an additional 24-h incubation period, cultures were harvested for DNA flow cytometry (Fig. 5). As expected, shRNA-mediated repression of CycG2 did not alter the cell cycle profile of untreated asynchronous HCT116 cultures but did significantly blunt the $G_2/M$ checkpoint accumulation of doxorubicin-treated HCT116 cells (Fig. 5, *A–C*). In contrast to cells expressing sh 1-B, HCT116 cells transfected with expression vectors for the non-silencing control (NSC) shRNA did not exhibit an abrogation of the $G_2/M$ checkpoint (Fig. 5A). Cells transfected with empty vector also exhibited a potent $G_2/M$ checkpoint arrest response to doxorubicin (Fig. 5A). Statistical analyses indicated that KD of CycG2 in HCT116 cells results in a significant ($p < 0.001$) blunting of the drug-induced $G_2$-phase arrest response (Fig. 5B). To determine whether the $G_2/M$ checkpoint attenuation by shRNAs targeting the conserved Ex4.2/1-B site
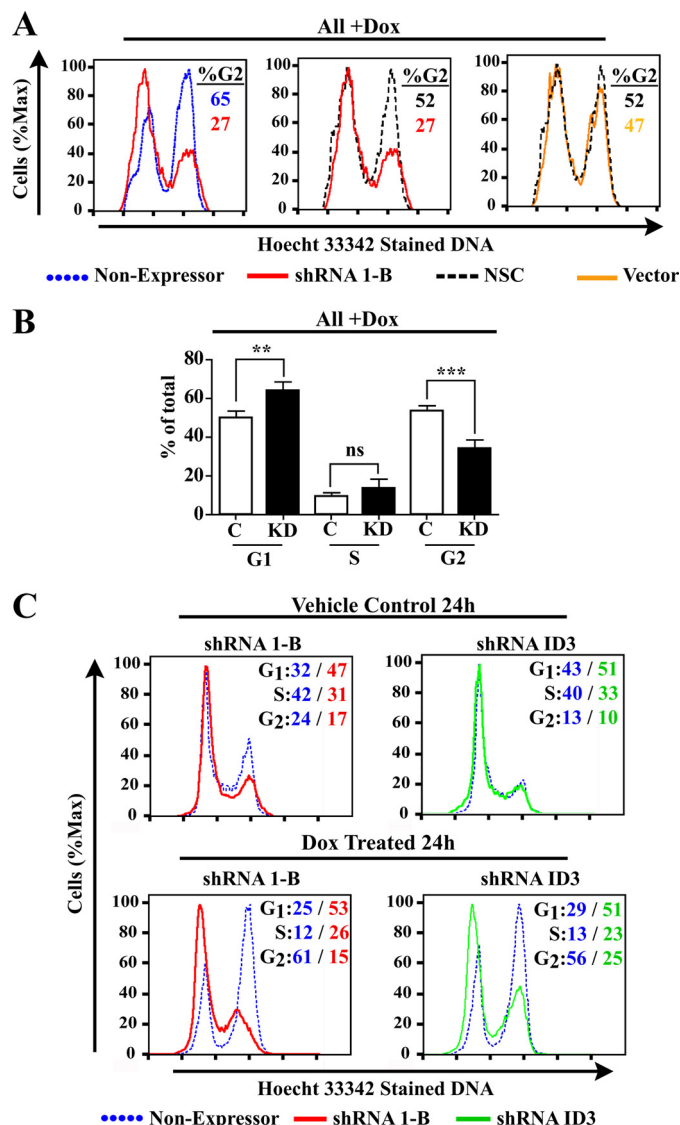


FIGURE 5. **shRNA-mediated knockdown of CycG2 inhibits doxorubicin-induced $G_2$-phase cell cycle arrest.** *A*, shown is a histogram overlay of DNA content in GFP-expressing populations of 24-h Dox-treated HCT116 cultures transfected 72 h earlier with control (*NSC* or *empty vector*) or CycG2 targeting (*1-B*) shRNA expression plasmids. Shown are non-expressing cells (*blue-dotted line*) and cells expressing specific shRNA 1-B (*red line*), the corresponding NSC (*black dashed-line*), or empty vector (*vector, orange line*). Hoechst staining of TOPRO negative cells was used to measure DNA content. The percentage of cells in each $G_2$ phase is shown in the *upper right corner* in the corresponding histogram. *B*, shown is a *bar graph* of the percentage of cells in $G_1$, S, and $G_2$ phases of the cell cycle for cells transfected with either control (*C*) or shRNA 1-B (*KD*) plasmids. Statistical analysis (one-way ANOVA with Bonferroni's post hoc test) of data from three independent experiments is shown (*** indicates $p < 0.001$, ** indicates $p < 0.01$). *ns*, not significant. *C*, shown is comparative cell cycle analysis of vehicle control or Dox-treated HCT116 cells transfected with indicated plasmids. Shown is DNA content in non-expressing cells of each culture (*blue-dotted line*) and cells expressing the shRNA 1-B (*red line*) or shRNA ID3 (*green line*). Percentage of cells in each phase of the cell cycle is shown at the *right of each overlay* in color-coded type corresponding to the respective histogram.

could be reproduced with shRNAs targeting another *CCNG2*-specific site, we tested the effect that doxorubicin treatment had on HCT116 cells expressing the ID3 shRNA construct (Fig. 5C). As with expression of sh 1-B shRNA, suppression of *CCNG2* via transient transfection with the ID3 shRNA construct did not alter the cell cycle distribution of untreated
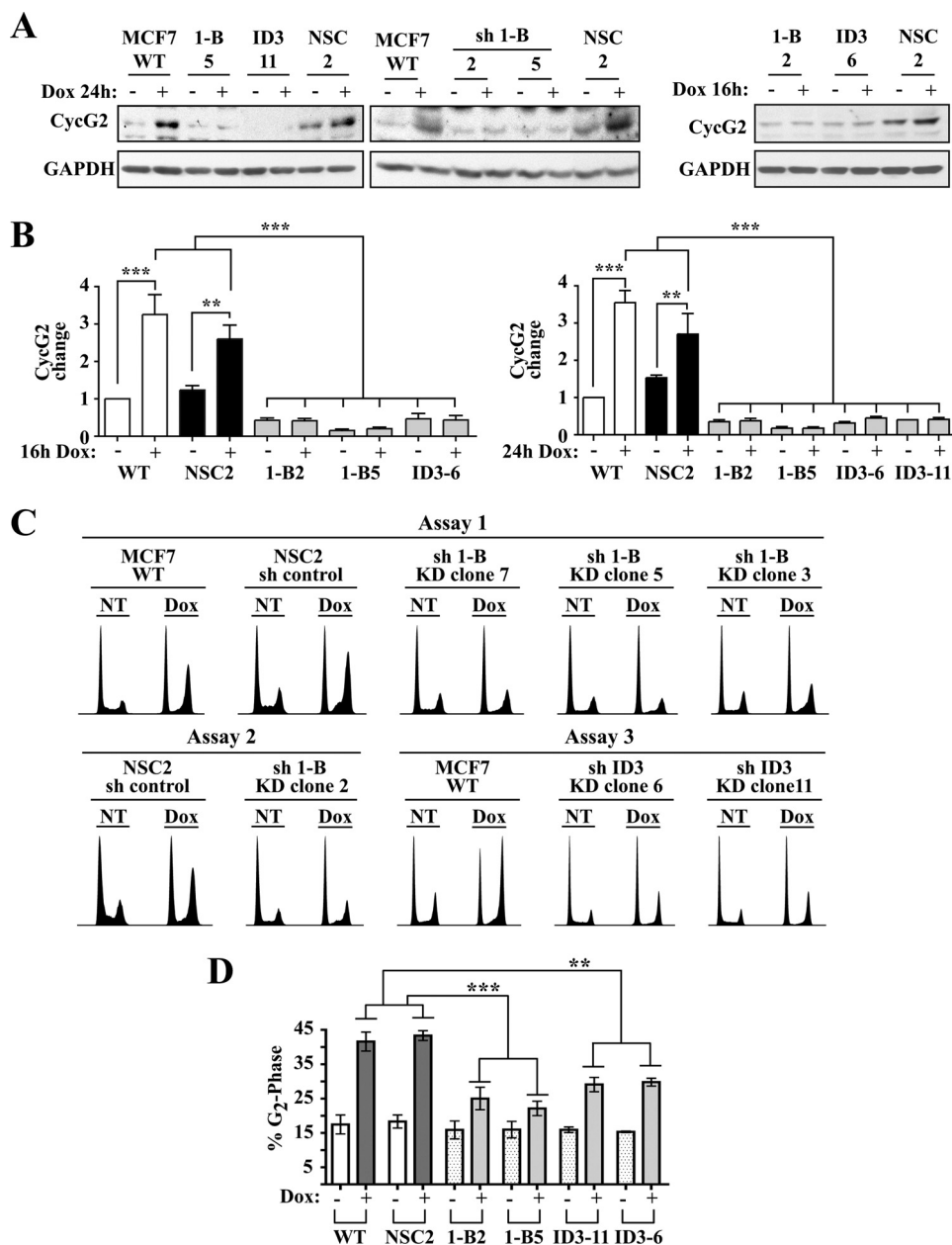
FIGURE 6. **Stable knockdown of CycG2 blunts the G$_2$-phase checkpoint response of MCF7 cells to doxorubicin.** *A* and *B*, shown is an immunoblot assessment of endogenous CycG2 levels relative to loading control. *A*, shown is endogenous CycG2 expression in the indicated cultures treated for 24 h (*left*) or 16 h (*right*) with doxorubicin (*Dox*, +) or vehicle alone (−). *B*, shown is a *bar graph* and statistical analysis (one-way ANOVA with Bonferroni's post hoc test) of -fold increase in CycG2 expression in cultures of MCF7 WT, NSC control, and CycG2 KD clones treated (+) with Dox or vehicle (−) for 16 h (*left*) or 24 h (*right*) (*** indicates $p < 0.001$, ** indicates $p < 0.01$). *C*, DNA flow cytometry analysis of cell cycle profiles in MCF7 WT, NCS control, and CycG2 KD clones after 24 h of exposure to Dox or mock (*NT*) treatments. *D*, statistical analysis of the average percentage of cells in G$_2$/M phase of the indicated Dox treated (+) and non-treated (−) cultures (one-way ANOVA with Tukey's post hoc, ***, $p < 0.001$; **, $p < 0.01$).

HCT116 cells but did potently repress the doxorubicin-induced accumulation of cells at the G$_2$/M checkpoint (Fig. 5*C*). Taken together our results strongly suggested that loss of CycG2 alters the G$_2$/M checkpoint arrest response of cells to doxorubicin.

*Stable Expression of CycG2-targeting shRNAs Attenuates Doxorubicin-induced G$_2$-phase Checkpoint Responses in MCF7 Cells*—As CycG2 has been implicated as an important biomarker for breast cancers (16, 20, 30), we sought to determine whether CycG2 contributes to the DNA damage checkpoint response of MCF7 breast cancer cells to doxorubicin. Puromy-

cin-resistant clones of MCF7 cells stably harboring vectors encoding sh 1-B, NSC, and ID3 shRNAs were established and characterized (Fig. 6 and supplemental Fig. S8). Immunoblot analysis determined that both exogenous (supplemental Fig. S8*A*) and endogenous human (Fig. 6, *A* and *B*) CycG2 expression were strongly repressed in clones containing expression cassettes for the CycG2-targeting shRNAs sh 1-B and ID3 but not in clones harboring the NSC control shRNA vector (Fig. 6, *A* and *B*). Importantly, in contrast to NSC and wild-type MCF7 controls, those shRNA-expressing clones exhibiting significant ($p < 0.001$) repression of doxorubicin-induced CycG2 levels
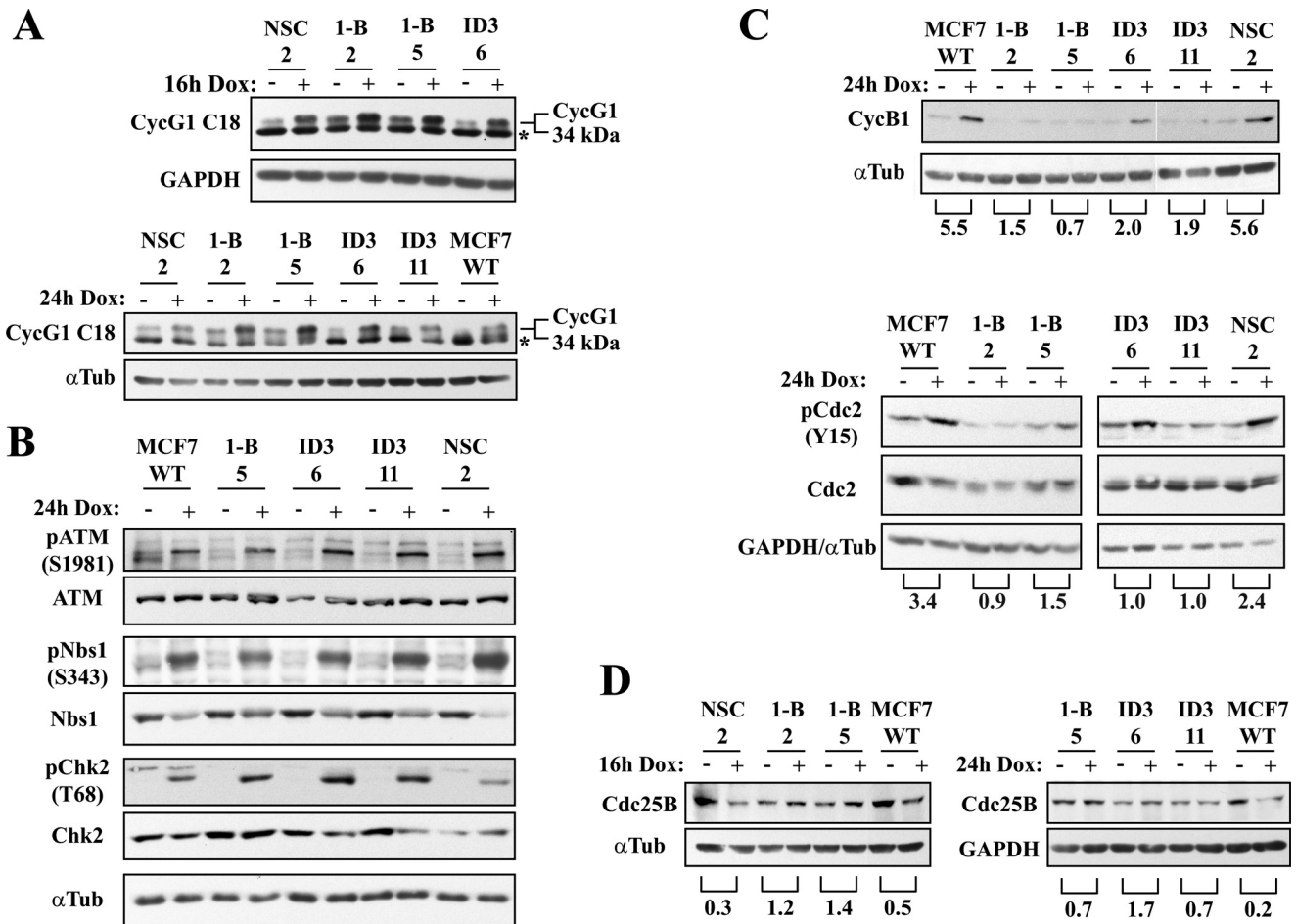
FIGURE 7. **Inhibition of CycG2 expression limits doxorubicin-induced accumulation of phospho-inhibited cyclin B/Cdc2 complexes.** *A–D,* shown is an immunoblot analysis of changes in protein expression induced by treatment of indicated MCF7 cultures with doxorubicin (*Dox*). *A,* expression of CycG1 compared with loading control GAPDH or $\alpha$-tubulin ($\alpha Tub$) after 16 h (*top*) or 24 h (*bottom*) of Dox treatment (* denotes a nonspecific background band). *B,* expression of pATM(S1981), pNbs1(Ser-343), and pChk2(Thr-68) compared with total ATM, Nbs1, Chk2, and loading control $\alpha$-tubulin in the indicated vehicle control (−) and Dox (+)-treated cultures. *C,* shown is CycB1 (*top*) and pCdc2(Tyr-15) (*bottom*) expression relative to loading control, $\alpha$-tubulin, or total Cdc2 (*bottom*) and GAPDH in the indicated cell populations. -Fold change in protein expression compared with untreated (−) controls is indicated under *brackets*. *D,* shown is immunoblot detection of Cdc25B relative to GAPDH in designated cultures. -Fold decrease in expression level compared with untreated (−) controls is indicated under *brackets*.

also showed an altered $G_2/M$ checkpoint arrest response to doxorubicin (Fig. 6, *C* and *D,* and supplemental Fig. S8*B*). This response was reproducible with multiple doxorubicin-treated CycG2 KD clones displaying a statistically significant (*p* values <0.01–0.001) reduction in the percentage of $G_2/M$-arrested cells (Fig. 6*D*).

Because the closest homolog of CycG2, CycG1, is a DNA damage response protein linked to regulation of $G_2/M$ transition (35–37), we assessed whether KD of CycG2 affected CycG1 expression (Fig. 7*A*). As predicted doxorubicin-induced DNA damage triggered up-regulation of CycG1 in MCF7 WT and NSC cells. Importantly, doxorubicin induction of CycG1 expression was maintained in all of the CycG2 KD clones (Fig. 7*A* and supplemental Fig. S9*A*). Given that ectopic CycG2-induced cell cycle arrest requires expression of Chk2 and p53 and promotes expression of the phospho-activated forms of Chk2 and Nbs1, we examined the effect CycG2 KD has on the expression of phospho-activated forms of these proteins (Fig. 7*B*). Notably, results indicated that, compared with the response in MCF7 WT and NSC control cells, depletion of CycG2 did not

appreciably effect the DNA damage response induction of phospho-Nbs1 or -Chk2 in the KD clones (Fig. 7*B*). Passage from $G_2$ phase into mitosis requires active CycB1-Cdc2 complexes, but once in mitosis cyclin B1 (CycB1) is targeted for proteasomal-mediated degradation (8). Importantly, DNA damage-induced accumulation of CycB1 observed in the doxorubicin-treated WT and NSC control cells was much reduced in the CycG2-KD clones (Fig. 7*C*), consistent with the relative reduction in the amount of cells arrested at the $G_2/M$ boundary (Fig. 6, *C* and *D*). DNA damage signaling is known to inhibit CycB1-Cdc2 activation through maintenance of the Wee1- and Myt1 kinase-mediated inhibitory phosphorylation of Cdc2 on Thr-14 and Thr-15 (8). Immunoblot analysis indicated that, in contrast to doxorubicin-treated cultures of control WT and NSC cells, Thr-15-phosphorylated Cdc2 levels were not strongly increased in drug-treated CycG2 KD clones (Fig. 7*C* and supplemental Fig. S9*C*).

Activation of Cdc2 is largely promoted through dephosphorylation of its inhibitory sites by the dual specificity phosphatases Cdc25B and Cdc25C. Consistent with the known effects of

genotoxic stress on Cdc25B expression levels (38–40), immunoblot analysis revealed reduced expression of Cdc25B in doxorubicin-treated, relative to untreated, MCF7 WT and NSC cells (Fig. 7D). Interestingly, extracts from doxorubicin-challenged CycG2 KD clones did not show a noticeable decrease in Cdc25B expression levels relative to the basal level in the respective undosed clone control (Fig. 7D). Rather, Cdc25B abundance in the doxorubicin-treated CycG2 KD clones appeared to be similar to or even increased above the level of its respective non-treated control. Although the basal level of Cdc25B in untreated cultures of CycG2 KD clones appeared lower than that in unperturbed MCF7 WT and NSC populations (Fig. 7D), the fact that this difference was not reflected by a respective increase in the percentage of CycG2 KD cells in $G_2$/M (Fig. 6, C and D and supplemental Fig. S8B) suggests that the CycG2 KD clones have adapted to this lower basal level. Contrasting the difference in modulation of Cdc25B by doxorubicin that was observed between the CycG2-expressing and KD populations (the latter showing no decrease in Cdc25B levels), Wee1 abundance, induction of phospho-inhibited Cdc25C and modulation of Cdc25C levels were comparable among all drug-treated populations; the doxorubicin-dosed MCF7 WT, NSC, and CycG2 KD clones all exhibited a similar expression pattern (data not shown). Taken together these results suggest that blocking CycG2 up-regulation during a DNA damage response to DSBs promotes activation of CycB1-Cdc2 complexes by hindering the DDR-induced down-regulation of Cdc25B expression.

*Doxorubicin-induced Up-regulation of Cyclin G2 Is ATM-independent*—To investigate the influence of ATM activity on CycG2 expression, we first tested whether pharmacological inhibition of ATM kinase activity blunts DNA damage-induced up-regulation of CycG2 levels (Fig. 8A). Consistent with previously reported effects of caffeine on ATM/ATR activity (41) and their target checkpoint kinases (42), treatment of MCF7 cultures with doxorubicin in the continual presence of 3 mM caffeine blunted the expression of pChk1(Ser-345) but not pChk2(Thr-68) (Fig. 8A). The later may be due to the ability of DNA-PK to phosphorylate Chk2 in the absence of ATM and ATR activity (43, 44). Importantly, we found that 3 mM caffeine also dampened the doxorubicin-induced elevation of CycG2 expression (Fig. 8A). Cotreatment of MCF7 cells with 10 μM of the more specific ATM inhibitor KU55933 (34) had no effect on doxorubicin-induced elevation of CycG2 expression but as expected (45, 46) did reduce the expression of Thr-68-phosphorylated Chk2 (Fig. 8A). These results suggest that DNA damage-mediated up-regulation of CycG2 expression does not require ATM activity.

To further investigate the relationship of CycG2 to ATM signaling, we tested the effects of doxorubicin on CycG2 expression and cell cycle progression in cells devoid of ATM function. Importantly, although ATM-deficient cells do not maintain a $G_1$-phase cell cycle arrest upon induction of DSBs, ATM-independent $G_2$/M checkpoint arrest responses to genotoxic stressors (including doxorubicin) do occur (47–51). As expected, culture of the ATM-deficient (AT) human fibroblast line GM05849 with doxorubicin for 24 h did not, in contrast to WT cells, arrest them in $G_1$ phase (Fig. 8B and supplemental Fig. S10) but did provoke a potent $G_2$/M checkpoint arrest
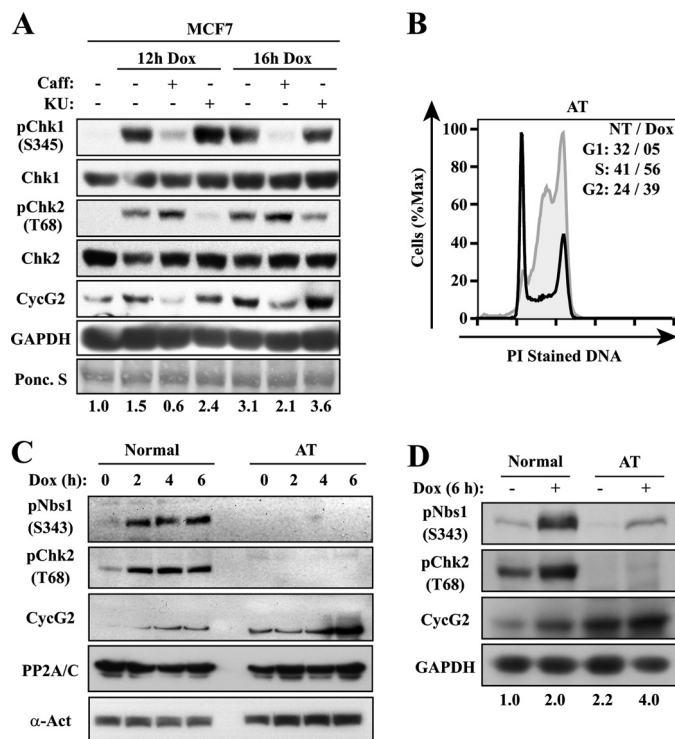


FIGURE 8. **Up-regulation of CycG2 during doxorubicin-induced DNA damage is caffeine-sensitive but does not require ATM.** *A*, shown is the influence of phosphoinositide 3-kinase-related kinase/ATM inhibitors caffeine (*Caff*) and KU55933 (*KU*) on doxorubicin (*Dox*)-induced DDR regulation of CycG2 levels in MCF7 cells assessed by immunoblotting. Increase or decrease in CycG2 expression relative to untreated control is indicated by *numbers below each lane*. *Ponc. S*, Ponceau S. *B*, histogram overlay of propidium iodide-stained DNA in ATM-deficient (*AT*) human fibroblasts after 24 h of culture with doxorubicin (*gray area*) compared with untreated mock control cells (*black line*) is shown. The percentage of untreated (*NT*) and doxorubicin-treated AT cells in each phase of the cell cycle is indicated at the *upper right*. *PI*, propidium iodide. *C* and *D*, shown is an immunoblot assessment of CycG2 expression relative to pNBS1(Ser-343), pChk2(Thr-68), and the loading control proteins α-actinin (*α-Act*) and PP2A/C in WT and AT fibroblasts cultured over a time course + or − doxorubicin (*C*). *D*, shown is CyG2 expression relative to GAPDH loading control in WT and AT cells cultured for 6 h in the presence (+) or absence (−) of doxorubicin. Note that although there is a reduced phospho-modification of Chk2 and Nbs1 in doxorubicin-treated AT compared with WT cells, doxorubicin treatment increased CycG2 expression ∼2-fold over the respective basal level for each culture.

response (Fig. 8B). To verify that doxorubicin-induced up-regulation of CycG2 is ATM-independent, WT and AT cells were cultured in the presence of 345 nM doxorubicin or vehicle control for 2, 4, or 6 h and assessed for activation of ATM pathway signaling and CycG2 expression (Fig. 8C). Immunoblot analysis of lysates from WT cultures indicated that, as expected, levels of phospho-activated forms of Nbs1 and Chk2 increased markedly within 2 h of doxorubicin treatment. As seen in other ATM competent cells (Figs. 3 and 4 and supplemental Figs. S5 and S6), up-regulation of CycG2 expression in AT cells was detectable within 4 h of exposure to doxorubicin, increasing 2-fold by 6 h of treatment (Fig. 8, C and D). Doxorubicin induction of pChk2(Thr-68) and pNbs1(Ser-343) expression in AT cultures was, as expected, nearly undetectable during the first 6 h of treatment. However, in contrast to the obvious deficiencies in the AT cell DDR, CycG2 expression was still up-regulated within 4 h of treatment, increasing nearly 2-fold by 6 h of treatment (Fig. 8, C and D). Notably, the basal level of CycG2 in AT

cells was higher than the basal level in the WT control (Fig. 8, *C* and *D*), indicating that increased basal expression of CycG2 is better tolerated in the absence of ATM. Nevertheless, doxorubicin did up-regulate CycG2 expression over basal levels to a similar degree in both WT and AT cells (Fig. 8, *C* and *D*). Collectively our results show that DDR induction of CycG2 expression is ATM-independent.

## DISCUSSION

*CCNG2* expression is up-regulated as cells undergo cell cycle arrest in response to a variety of growth inhibitory signals (9, 10, 12, 16 –19, 22, 24 –26). We previously showed that unscheduled CycG2 expression inhibits DNA synthesis, blunts CDK2 (but not CDK4) activity (13), and induces a p53-dependent $G_1$-phase cell cycle arrest (15). Similar results have since been replicated by others using various epitope-tagged forms of CycG2 in several cell lines (10, 13, 14, 16, 24). Here we show that the potent cell cycle arrest response of HCT116 cells to exogenous CycG2 requires intact alleles for Chk2 and p53 (Fig. 1). That loss of p21 only partially reduces CycG2-medited cell cycle inhibition suggests that additional effectors downstream of Chk2 or p53 are involved. Thr-68 phosphorylation of Chk2 by activated ATM triggers Chk2-mediated $G_1$ checkpoint arrest responses to DNA DSBs (6, 52). However, the $G_1$-phase cell cycle arrest response induced by ectopic CycG2 does not require ATM (Fig. 1). Consistent with the Chk2-dependent arrest, ectopic elevation of CycG2 also promoted the expression of the Thr-68 phospho-activated form of Chk2 (Fig. 2). Because phosphorylation of p53 by Chk2 is known to promote $G_1$-phase checkpoint arrest (53), and pChk2(Thr-68), but not pChk1(Ser-345) levels, were robustly elevated in CycG2-overexpressing WT and p53-deficient HCT116 cells (Fig. 2), the p53-dependent $G_1$-phase arrest induced by ectopic CycG2 is likely downstream of activated Chk2.

Unscheduled enforced expression of CycG2 in the absence of coordinated dsDNA DDR signaling ultimately has more profound effects on $G_1$/S compared to $G_2$/M transition. It is however unclear how CycG2 overexpression promotes expression of Thr-68 phospho-activated Chk2. As the CycG2-induced cell cycle arrest was independent of ATM, the effects of ectopic CycG2 on Chk2 are likely ATM-independent. That phosphorylation of the ATR target Chk1 was not promoted by ectopic CycG2 expression suggests that CycG2 overexpression did not activate ATR. Recent work indicates that pChk2(Thr-68) serves a DNA damage-independent function during mitosis to ensure proper spindle assembly and maintain chromosomal stability (54, 55). The kinases PLK1, TTK/hMps1, and DNA-PK can each interact with and phosphorylate Chk2 on Thr-68 and play DDR-independent roles in regulating mitosis and spindle assembly checkpoints (43, 52, 56 –58). Because ectopic CycG2 expression promotes formation of nocodazole-resistant microtubules and aberrant nuclei (13), its overexpression may trigger a defective mitosis that provokes Chk2 activation through one of these kinases. As cells exit mitosis this stress response could ultimately result in a $G_1$-phase arrest. Alternatively, as CycG2 can interact and form complexes with PP2A B56 and C subunits (13, 59) and phosphorylation of Chk2 on Thr-68 is negatively regulated by B56 isoforms of PP2A (60, 61), it is possible that in

otherwise unperturbed cells, overexpressed CycG2 acts as a PP2A sink and in so doing inhibits PP2A-mediated dephosphorylation of Chk2. In this context it is notable that CycG2, PP2A, and Chk2 all associate with centrosomes (15, 62, 63).

We explored the possibility that CycG2 contributes to cell cycle control during genotoxic stress-induced DDRs. Genotoxic topoisomerase II poisons (32) play a central role in cancer chemotherapies. Although doxorubicin and etoposide belong to distinctly different classes of chemotherapeutics (1, 32), both induce DNA DSBs by trapping topoisomerase II-DNA intermediates and provoke a potent $G_2$-phase checkpoint arrest in treated cells (1, 32). We found that endogenous CycG2 expression is increased up to 8-fold when cancer cells are cultured with doxorubicin or etoposide (Figs. 3 and 4 and supplemental Figs. S5 and S6). Concordant with the idea that CycG2 is up-regulated in response to activation of DNA DSB signaling pathways, previous studies indicated significant elevation of *CCNG2* mRNAs upon γ-irradiation-induced DNA damage (64). Because the doxorubicin-stimulated increase in CycG2 levels is clearly detectable within 4 h of dosing, well before an obvious arrest at the $G_2$/M boundary (Fig. 4 and supplemental Figs. S5 and S6), this likely reflects a DDR pathway triggered up-regulation of CycG2 and not the simple accumulation of a cell cycle phase-dependent protein. That the continuous rise in CycG2 levels followed activation of ATM signaling by several hours and persisted for up to 24 h suggested that CycG2 may play a role in the maintenance of $G_2$/M checkpoint arrest. Indeed, through transient and stable transfection of CycG2-targeting shRNA expression constructs, we determined that CycG2 contributes to the doxorubicin-induced $G_2$/M checkpoint arrest response of NIH3T3, HCT116, and MCF7 cells (Fig. 5–7 and supplemental Figs. S7 and S8).

Doxorubicin-induced DNA damage triggers ATM and ATR activation (1, 32). Although ATR and ATM both enforce the DSB DDR delay in M-phase entry, ATR activity is thought to regulate the majority of the late (2–9 h post γ-irradiation) phase of the checkpoint response (4, 46, 65). In the absence of ATM, both ATR and DNA-PK regulate DNA DSB $G_2$/M checkpoint responses (50, 51). We showed (Fig. 8*A*) that doxorubicin induction of CycG2 (and Chk1 phosphorylation) in MCF7 cells is not blocked by 10 $\mu$M of the ATM inhibitor KU55933 (ATM $IC_{50} = 13$ nM, ATR $IC_{50} > 100$ $\mu$M (34)) but is blunted by 3 mM caffeine (ATM $IC_{50} = 0.2$ mM, ATR $IC_{50} = 1.1$ mM). Moreover, we determined that this genotoxic stress elevates CycG2 expression to a similar degree in WT and ATM-deficient fibroblasts (Fig. 8, *B* and *C*). Thus, doxorubicin-triggered CycG2 up-regulation does not require early ATM-initiated signaling.

The concentration of caffeine that repressed CycG2 expression is within the $IC_{50}$ range for ATR (1.1 mM) and mTOR (0.4 mM) but severalfold lower than the $IC_{50}$ for DNA-PK (10 mM) (41). Because direct inhibition of mTOR (via rapamycin) promotes rather than represses CycG2 expression (16, 19, 66), the ability of 3 mM caffeine to repress doxorubicin-induced up-regulation of CycG2 is most likely independent of its effects on mTOR. In contrast to KU55933, caffeine did not diminish pChk2(Thr-68) levels in doxorubicin-treated MCF7 cells. However, caffeine-insensitive DNA damage induction of Chk2

phosphorylation has been reported by others (47, 67–69). DNA-PK activity is sensitive to KU55933 ($IC_{50} = 2.5\ \mu M$), but 10 $\mu M$ KU55933 did not blunt doxorubicin-induced CycG2 expression, suggesting that this response is DNA-PK-independent. The late-phase DDR increase in CycG2 levels coupled with its ATM independence and caffeine sensitivity, suggests that doxorubicin-induced CycG2 up-regulation is ATR-dependent; however, we cannot exclude DNA-PK involvement.

The *CCNG1* gene encoding the closest CycG2 homolog, CycG1, is a direct transcriptional target of p53, and its transcript levels increase severalfold in response to DNA damage (25, 27, 28, 70). Predictably, CycG1 expression was significantly up-regulated in doxorubicin-treated MCF7 cells (Figs. 7*A* and supplemental Fig. S9). Importantly we found that doxorubicin-induced DDR elevation of endogenous CycG1 expression was unaffected by shRNA-mediated KD of CycG2, further indicating the specificity of our *CCNG2*-targeting shRNA constructs. CycG1 has been linked to $G_2/M$ checkpoint control (35–37); however, whether it promotes or inhibits either cell cycle arrest or cell death in response to DNA damage is controversial (35–37, 70–72). Because CycG2 depleted cells exhibited a reduced $G_2/M$ checkpoint despite the rise in CycG1 levels suggests that CycG1 does not compensate for loss of CycG2 and that these two homologs do not serve fully redundant functions.

In variance with the effects of ectopic CycG2 expression on Chk2, shRNA-mediated blunting of CycG2 in MCF7 cells had no affect on the DDR-induced elevation of pChk2(Thr-68) (Fig. 7*B*). CycB1 expression levels are normally increased as cells enter $G_2$ phase and decreased as cells proceed through mitosis (8). As predicted, the doxorubicin-triggered $G_2/M$ checkpoint led to accumulation of CycB1 levels in WT and shRNA control cultures. In contrast, CycG2 KD clones did not show increased CycB1 expression under the same conditions (Fig. 7*C*). In accord with their blunted $G_2/M$ checkpoint arrest response, doxorubicin-treated CycG2 KD clones also exhibited diminished levels of phospho-inhibited Cdc2 when compared with treated WT and shRNA controls (Fig. 7*C*). Inhibitory phosphorylation of Cdc2 on Thr-14 and Thr-15 by the Myt1 and Wee1 kinases is counterbalanced by the Cdc25 phosphatases that dephosphorylate these sites (6, 8). During DDR signaling the dual specificity phosphatases Cdc25B and Cdc25C are themselves subject to Chk1 and Chk2 inhibitory phosphorylation that promotes Cdc25 degradation and/or restricted subcellular localization (8). Although Cdc25B expression is not required for $G_2/M$ transition in otherwise unperturbed somatic cell populations, it is essential for resumption of cell cycle progression after DNA damage-induced checkpoint arrest (8). We found that Cdc25B levels were diminished in doxorubicin-treated compared with mock-treated WT and NSC cells, but no such doxorubicin-induced decrease from base-line levels was apparent for the CycG2 KD clones. Given that increasing Cdc25B expression levels even moderately impairs $G_2/M$ checkpoint control (39, 73, 74), our results (Figs. 6 and 7) suggest that the weakened $G_2/M$ checkpoint arrest in CycG2 KD cells is due to a disruption of the regulatory circuit controlling Cdc25B expression. Thus, CycG2 may contribute to $G_2/M$ checkpoint enforcement by constraining the Cdc25B/CycB1-Cdc2 axis.

*CCNG2* transcripts are up-regulated during $G_1$-phase cell cycle arrest responses to a variety of DDR-independent antimitogenic signaling cascades (9, 12, 16, 17). RNAi KD of *CCNG2* has been shown to blunt the $G_1$-phase arrest response to some of these growth inhibitory signals (14, 17). Given these observations and the effects that ectopic CycG2 expression has on $G_1/S$ phase transition, the diminished $G_2/M$ checkpoint arrest response of CycG2 KD cells to doxorubicin was somewhat surprising. However, such seemingly contradictory findings are not unprecedented for cell cycle inhibitors and have been described for both p53 and p21 (75–79). Although most of the evidence in the literature supports a role for CycG2 in limiting $G_1/S$-phase transition, there are indications that CycG2 could participate in $G_2/M$ regulation (30, 80–83). The idea that CycG2 has a regulatory function in $G_2/M$-phase transition is also supported by the discovery that CycG2 is a substrate of the anaphase promoting complex (APC), being both ubiquitinated and degraded in mitotic cell extracts enriched with APC-Cdc20 complexes (84). Consistent with the notion that CycG2 helps restrict $G_2/M$ transition, we show for the first time that 1) a caffeine-sensitive but KU55933-insensitive and ATM-independent DDR pathway promotes CycG2 up-regulation during the late phase of doxorubicin-induced $G_2/M$ checkpoint and 2) that CycG2 depletion attenuates $G_2/M$ checkpoint-induced down-regulation of Cdc25B, inhibitory phosphorylation of Cdc2, and accumulation of CycB1. Given the report that elevated CycG1 expression promotes transcriptional activation of CycB1 and abrogation of $G_2/M$ checkpoint arrest (72), it is possible that there is a Yin and Yang relationship between these two G-type cyclins and that CycG2 acts to restrict CycG1-associated activity during DNA damage responses. The single CycG homolog in *Drosophila* is an essential protein for embryonic development that restricts cell proliferation and growth (85). Whether the two mammalian CycG paralogs evolved to serve opposing or complementary functions is an open question. Future studies will be needed to determine the exact mechanism by which CycG2 modulates the Cdc25B-Cdc2/CycB1 regulatory loop during $G_2/M$ checkpoint.

## REFERENCES

1. Jackson, S. P., and Bartek, J. (2009) The DNA-damage response in human biology and disease. *Nature* **461,** 1071–1078
2. Lovejoy, C. A., and Cortez, D. (2009) Common mechanisms of PIKK regulation. *DNA Repair* **8,** 1004–1008
3. Derheimer, F. A., and Kastan, M. B. (2010) Multiple roles of ATM in monitoring and maintaining DNA integrity. *FEBS Lett.* **584,** 3675–3681
4. Shiotani, B., and Zou, L. (2009) ATR signaling at a glance. *J. Cell Sci.* **122,**

301–304

5. Hill, R., and Lee, P. W. (2010) The DNA-dependent protein kinase (DNA-PK). More than just a case of making ends meet? *Cell Cycle* **9,** 3460–3469

6. Stracker, T. H., Usui, T., and Petrini, J. H. (2009) Taking the time to make important decisions. The checkpoint effector kinases Chk1 and Chk2 and the DNA damage response. *DNA Repair* **8,** 1047–1054

7. Jazayeri, A., Falck, J., Lukas, C., Bartek, J., Smith, G. C., Lukas, J., and Jackson, S. P. (2006) ATM- and cell cycle-dependent regulation of ATR in response to DNA double-strand breaks. *Nat. Cell Biol.* **8,** 37–45

8. Lindqvist, A., Rodríguez-Bravo, V., and Medema, R. H. (2009) The decision to enter mitosis. Feedback and redundancy in the mitotic entry network. *J. Cell Biol.* **185,** 193–202

9. Martínez-Gac, L., Marqués, M., García, Z., Campanero, M. R., and Carrera, A. C. (2004) Control of cyclin G2 mRNA expression by forkhead transcription factors. Novel mechanism for cell cycle control by phosphoinositide 3-kinase and forkhead. *Mol. Cell. Biol.* **24,** 2181–2189

10. Chen, J., Yusuf, I., Andersen, H. M., and Fruman, D. A. (2006) FOXO transcription factors cooperate with δEF1 to activate growth suppressive genes in B lymphocytes. *J. Immunol.* **176,** 2711–2721

11. Horne, M. C., Goolsby, G. L., Donaldson, K. L., Tran, D., Neubauer, M., and Wahl, A. F. (1996) Cyclin G1 and cyclin G2 comprise a new family of cyclins with contrasting tissue-specific and cell cycle-regulated expression. *J. Biol. Chem.* **271,** 6050–6061

12. Horne, M. C., Donaldson, K. L., Goolsby, G. L., Tran, D., Mulheisen, M., Hell, J. W., and Wahl, A. F. (1997) Cyclin G2 is up-regulated during growth inhibition and B cell antigen receptor-mediated cell cycle arrest. *J. Biol. Chem.* **272,** 12650–12661

13. Bennin, D. A., Don, A. S., Brake, T., McKenzie, J. L., Rosenbaum, H., Ortiz, L., DePaoli-Roach, A. A., and Horne, M. C. (2002) Cyclin G2 associates with protein phosphatase 2A catalytic and regulatory B' subunits in active complexes and induces nuclear aberrations and a $G_1/S$ phase cell cycle arrest. *J. Biol. Chem.* **277,** 27449–27467

14. Kim, Y., Shintani, S., Kohno, Y., Zhang, R., and Wong, D. T. (2004) Cyclin G2 dysregulation in human oral cancer. *Cancer Res.* **64,** 8980–8986

15. Arachchige Don, A. S., Dallapiazza, R. F., Bennin, D. A., Brake, T., Cowan, C. E., and Horne, M. C. (2006) Cyclin G2 is a centrosome-associated nucleocytoplasmic shuttling protein that influences microtubule stability and induces a p53-dependent cell cycle arrest. *Exp. Cell Res.* **312,** 4181–4204

16. Le, X. F., Arachchige-Don, A. S., Mao, W., Horne, M. C., and Bast, R. C., Jr. (2007) Roles of human epidermal growth factor receptor 2, c-Jun $NH_2$-terminal kinase, phosphoinositide 3-kinase, and p70 S6 kinase pathways in regulation of cyclin G2 expression in human breast cancer cells. *Mol. Cancer Ther.* **6,** 2843–2857

17. Xu, G., Bernaudo, S., Fu, G., Lee, D. Y., Yang, B. B., and Peng, C. (2008) Cyclin G2 is degraded through the ubiquitin-proteasome pathway and mediates the antiproliferative effect of activin receptor-like kinase 7. *Mol. Biol. Cell* **19,** 4968–4979

18. Tran, H., Brunet, A., Grenier, J. M., Datta, S. R., Fornace, A. J., Jr., DiStefano, P. S., Chiang, L. W., and Greenberg, M. E. (2002) DNA repair pathway stimulated by the forkhead transcription factor FOXO3a through the Gadd45 protein. *Science* **296,** 530–534

19. Grolleau, A., Bowman, J., Pradet-Balade, B., Puravs, E., Hanash, S., Garcia-Sanz, J. A., and Beretta, L. (2002) Global and specific translational control by rapamycin in T cells uncovered by microarrays and proteomics. *J. Biol. Chem.* **277,** 22175–22184

20. Frasor, J., Danes, J. M., Komm, B., Chang, K. C., Lyttle, C. R., and Katzenellenbogen, B. S. (2003) Profiling of estrogen up- and down-regulated gene expression in human breast cancer cells. Insights into gene networks and pathways underlying estrogenic control of proliferation and cell phenotype. *Endocrinology* **144,** 4562–4574

21. Oliver, T. G., Grasfeder, L. L., Carroll, A. L., Kaiser, C., Gillingham, C. L., Lin, S. M., Wickramasinghe, R., Scott, M. P., and Wechsler-Reya, R. J. (2003) Transcriptional profiling of the Sonic hedgehog response. A critical role for N-myc in proliferation of neuronal precursors. *Proc. Natl. Acad. Sci. U.S.A.* **100,** 7331–7336

22. Murray, J. I., Whitfield, M. L., Trinklein, N. D., Myers, R. M., Brown, P. O., and Botstein, D. (2004) Diverse and specific gene expression responses to stresses in cultured human cells. *Mol. Biol. Cell* **15,** 2361–2374

23. Zhu, X., Hart, R., Chang, M. S., Kim, J. W., Lee, S. Y., Cao, Y. A., Mock, D., Ke, E., Saunders, B., Alexander, A., Grossoehme, J., Lin, K. M., Yan, Z., Hsueh, R., Lee, J., Scheuermann, R. H., Fruman, D. A., Seaman, W., Subramaniam, S., Sternweis, P., Simon, M. I., and Choi, S. (2004) Analysis of the major patterns of B cell gene expression changes in response to short-term stimulation with 33 single ligands. *J. Immunol.* **173,** 7141–7149

24. Fang, J., Menon, M., Kapelle, W., Bogacheva, O., Bogachev, O., Houde, E., Browne, S., Sathyanarayana, P., and Wojchowski, D. M. (2007) EPO modulation of cell-cycle regulatory genes and cell division in primary bone marrow erythroblasts. *Blood* **110,** 2361–2370

25. Bates, S., Rowan, S., and Vousden, K. H. (1996) Characterization of human cyclin G1 and G2. DNA damage inducible genes. *Oncogene* **13,** 1103–1109

26. Gajate, C., An, F., and Mollinedo, F. (2002) Differential cytostatic and apoptotic effects of ecteinascidin-743 in cancer cells. Transcription-dependent cell cycle arrest and transcription-independent JNK and mitochondrial mediated apoptosis. *J. Biol. Chem.* **277,** 41580–41589

27. Okamoto, K., and Beach, D. (1994) Cyclin G is a transcriptional target of the p53 tumor suppressor protein. *EMBO J.* **13,** 4816–4822

28. Zauberman, A., Lupo, A., and Oren, M. (1995) Identification of p53 target genes through immune selection of genomic DNA. The cyclin G gene contains two distinct p53 binding sites. *Oncogene* **10,** 2361–2366

29. Jensen, M. R., Audolfsson, T., Keck, C. L., Zimonjic, D. B., and Thorgeirsson, S. S. (1999) Gene structure and chromosomal localization of mouse cyclin G2 (Ccng2). *Gene* **230,** 171–180

30. Adorno, M., Cordenonsi, M., Montagner, M., Dupont, S., Wong, C., Hann, B., Solari, A., Bobisse, S., Rondina, M. B., Guzzardo, V., Parenti, A. R., Rosato, A., Bicciato, S., Balmain, A., and Piccolo, S. (2009) A mutant-p53/Smad complex opposes p63 to empower TGFβ-induced metastasis. *Cell* **137,** 87–98

31. Ito, Y., Yoshida, H., Uruno, T., Nakano, K., Takamura, Y., Miya, A., Kobayashi, K., Yokozawa, T., Matsuzuka, F., Kuma, K., and Miyauchi, A. (2003) Decreased expression of cyclin G2 is significantly linked to the malignant transformation of papillary carcinoma of the thyroid. *Anticancer Res.* **23,** 2335–2338

32. Nitiss, J. L. (2009) Targeting DNA topoisomerase II in cancer chemotherapy. *Nat. Rev. Cancer* **9,** 338–350

33. Zhao, L., Samuels, T., Winckler, S., Korgaonkar, C., Tompkins, V., Horne, M. C., and Quelle, D. E. (2003) Cyclin G1 has growth inhibitory activity linked to the ARF-Mdm2-p53 and pRb tumor suppressor pathways. *Mol. Cancer Res.* **1,** 195–206

34. Hickson, I., Zhao, Y., Richardson, C. J., Green, S. J., Martin, N. M., Orr, A. I., Reaper, P. M., Jackson, S. P., Curtin, N. J., and Smith, G. C. (2004) Identification and characterization of a novel and specific inhibitor of the ataxia-telangiectasia mutated kinase ATM. *Cancer Res.* **64,** 9152–9159

35. Shimizu, A., Nishida, J., Ueoka, Y., Kato, K., Hachiya, T., Kuriaki, Y., and Wake, N. (1998) CyclinG contributes to $G_2/M$ arrest of cells in response to DNA damage. *Biochem. Biophys. Res. Commun.* **242,** 529–533

36. Kimura, S. H., Ikawa, M., Ito, A., Okabe, M., and Nojima, H. (2001) Cyclin G1 is involved in $G_2/M$ arrest in response to DNA damage and in growth control after damage recovery. *Oncogene* **20,** 3290–3300

37. Kimura, S. H., and Nojima, H. (2002) Cyclin G1 associates with MDM2 and regulates accumulation and degradation of p53 protein. *Genes Cells* **7,** 869–880

38. Miyata, H., Doki, Y., Yamamoto, H., Kishi, K., Takemoto, H., Fujiwara, Y., Yasuda, T., Yano, M., Inoue, M., Shiozaki, H., Weinstein, I. B., and Monden, M. (2001) Overexpression of CDC25B overrides radiation-induced G2-M arrest and results in increased apoptosis in esophageal cancer cells. *Cancer Res.* **61,** 3188–3193

39. Bansal, P., and Lazo, J. S. (2007) Induction of Cdc25B regulates cell cycle resumption after genotoxic stress. *Cancer Res.* **67,** 3356–3363

40. Lemaire, M., Ducommun, B., and Nebreda, A. R. (2010) UV-induced down-regulation of the CDC25B protein in human cells. *FEBS Lett.* **584,** 1199–1204

41. Sarkaria, J. N., Busby, E. C., Tibbetts, R. S., Roos, P., Taya, Y., Karnitz, L. M., and Abraham, R. T. (1999) Inhibition of ATM and ATR kinase activities by the radiosensitizing agent, caffeine. *Cancer Res.* **59,** 4375–4382

42. Zhao, H., and Piwnica-Worms, H. (2001) ATR-mediated checkpoint

pathways regulate phosphorylation and activation of human Chk1. *Mol. Cell. Biol.* **21,** 4129–4139

43. Li, J., and Stern, D. F. (2005) Regulation of CHK2 by DNA-dependent protein kinase. *J. Biol. Chem.* **280,** 12041–12050

44. McSherry, T. D., and Mueller, P. R. (2004) *Xenopus* Cds1 is regulated by DNA-dependent protein kinase and ATR during the cell cycle checkpoint response to double-stranded DNA ends. *Mol. Cell. Biol.* **24,** 9968–9985

45. Rainey, M. D., Charlton, M. E., Stanton, R. V., and Kastan, M. B. (2008) Transient inhibition of ATM kinase is sufficient to enhance cellular sensitivity to ionizing radiation. *Cancer Res.* **68,** 7466–7474

46. Shiotani, B., and Zou, L. (2009) Single-stranded DNA orchestrates an ATM-to-ATR switch at DNA breaks. *Mol. Cell* **33,** 547–558

47. Théard, D., Coisy, M., Ducommun, B., Concannon, P., and Darbon, J. M. (2001) Etoposide and adriamycin but not genistein can activate the checkpoint kinase Chk2 independently of ATM/ATR. *Biochem. Biophys. Res. Commun.* **289,** 1199–1204

48. Xu, B., Kim, S. T., Lim, D. S., and Kastan, M. B. (2002) Two molecularly distinct $G_2$/M checkpoints are induced by ionizing irradiation. *Mol. Cell. Biol.* **22,** 1049–1059

49. Siu, W. Y., Lau, A., Arooz, T., Chow, J. P., Ho, H. T., and Poon, R. Y. (2004) Topoisomerase poisons differentially activate DNA damage checkpoints through ataxia-telangiectasia mutated-dependent and -independent mechanisms. *Mol. Cancer Ther.* **3,** 621–632

50. Arlander, S. J., Greene, B. T., Innes, C. L., and Paules, R. S. (2008) DNA protein kinase-dependent $G_2$ checkpoint revealed following knockdown of ataxia-telangiectasia mutated in human mammary epithelial cells. *Cancer Res.* **68,** 89–97

51. Tomimatsu, N., Mukherjee, B., and Burma, S. (2009) Distinct roles of ATR and DNA-PKcs in triggering DNA damage responses in ATM-deficient cells. *EMBO Rep.* **10,** 629–635

52. Chen, Y., and Poon, R. Y. (2008) The multiple checkpoint functions of CHK1 and CHK2 in maintenance of genome stability. *Front Biosci.* **13,** 5016–5029

53. Chehab, N. H., Malikzay, A., Appel, M., and Halazonetis, T. D. (2000) Chk2/hCds1 functions as a DNA damage checkpoint in $G_1$ by stabilizing p53. *Genes Dev.* **14,** 278–288

54. Stolz, A., Ertych, N., Kienitz, A., Vogel, C., Schneider, V., Fritz, B., Jacob, R., Dittmar, G., Weichert, W., Petersen, I., and Bastians, H. (2010) The CHK2-BRCA1 tumorsuppressor pathway ensures chromosomal stability in human somatic cells. *Nat. Cell Biol.* **12,** 492–499

55. Chabalier-Taste, C., Racca, C., Dozier, C., and Larminat, F. (2008) BRCA1 is regulated by Chk2 in response to spindle damage. *Biochim. Biophys. Acta* **1783,** 2223–2233

56. Tsvetkov, L., Xu, X., Li, J., and Stern, D. F. (2003) Polo-like kinase 1 and Chk2 interact and co-localize to centrosomes and the midbody. *J. Biol. Chem.* **278,** 8468–8475

57. Wei, J. H., Chou, Y. F., Ou, Y. H., Yeh, Y. H., Tyan, S. W., Sun, T. P., Shen, C. Y., and Shieh, S. Y. (2005) TTK/hMps1 participates in the regulation of DNA damage checkpoint response by phosphorylating CHK2 on threonine 68. *J. Biol. Chem.* **280,** 7748–7757

58. Lee, K. J., Lin, Y. F., Chou, H. Y., Yajima, H., Fattah, K. R., Lee, S. C., and Chen, B. P. (2011) Involvement of DNA-dependent protein kinase in normal cell cycle progression through mitosis. *J. Biol. Chem.* **286,** 12796–12802

59. Rual, J. F., Venkatesan, K., Hao, T., Hirozane-Kishikawa, T., Dricot, A., Li, N., Berriz, G. F., Gibbons, F. D., Dreze, M., Ayivi-Guedehoussou, N., Klitgord, N., Simon, C., Boxem, M., Milstein, S., Rosenberg, J., Goldberg, D. S., Zhang, L. V., Wong, S. L., Franklin, G., Li, S., Albala, J. S., Lim, J., Fraughton, C., Llamosas, E., Cevik, S., Bex, C., Lamesch, P., Sikorski, R. S., Vandenhaute, J., Zoghbi, H. Y., Smolyar, A., Bosak, S., Sequerra, R., Doucette-Stamm, L., Cusick, M. E., Hill, D. E., Roth, F. P., and Vidal, M. (2005) Toward a proteome-scale map of the human protein-protein interaction network. *Nature* **437,** 1173–1178

60. Freeman, A. K., Dapic, V., and Monteiro, A. N. (2010) Negative regulation of CHK2 activity by protein phosphatase 2A is modulated by DNA damage. *Cell Cycle* **9,** 736–747

61. Carlessi, L., Buscemi, G., Fontanella, E., and Delia, D. (2010) A protein phosphatase feedback mechanism regulates the basal phosphorylation of

Chk2 kinase in the absence of DNA damage. *Biochim. Biophys. Acta* **1803,** 1213–1223

62. Bollen, M., Gerlich, D. W., and Lesage, B. (2009) Mitotic phosphatases. From entry guards to exit guides. *Trends Cell Biol.* **19,** 531–541

63. Golan, A., Pick, E., Tsvetkov, L., Nadler, Y., Kluger, H., and Stern, D. F. (2010) Centrosomal Chk2 in DNA damage responses and cell cycle progression. *Cell Cycle* **9,** 2647–2656

64. Tsai, M. H., Chen, X., Chandramouli, G. V., Chen, Y., Yan, H., Zhao, S., Keng, P., Liber, H. L., Coleman, C. N., Mitchell, J. B., and Chuang, E. Y. (2006) Transcriptional responses to ionizing radiation reveal that p53R2 protects against radiation-induced mutagenesis in human lymphoblastoid cells. *Oncogene* **25,** 622–632

65. Brown, E. J., and Baltimore, D. (2003) Essential and dispensable roles of ATR in cell cycle arrest and genome maintenance. *Genes Dev.* **17,** 615–628

66. Zhou, J., Su, P., Wang, L., Chen, J., Zimmermann, M., Genbacev, O., Afonja, O., Horne, M. C., Tanaka, T., Duan, E., Fisher, S. J., Liao, J., Chen, J., and Wang, F. (2009) mTOR supports long term self-renewal and suppresses mesoderm and endoderm activities of human embryonic stem cells. *Proc. Natl. Acad. Sci. U.S.A.* **106,** 7840–7845

67. Darbon, J. M., Penary, M., Escalas, N., Casagrande, F., Goubin-Gramatica, F., Baudouin, C., and Ducommun, B. (2000) Distinct Chk2 activation pathways are triggered by genistein and DNA-damaging agents in human melanoma cells. *J. Biol. Chem.* **275,** 15363–15369

68. Wang, X. Q., Stanbridge, E. J., Lao, X., Cai, Q., Fan, S. T., and Redpath, J. L. (2007) p53-dependent Chk1 phosphorylation is required for maintenance of prolonged $G_2$ arrest. *Radiat. Res.* **168,** 706–715

69. Landsverk, K. S., Patzke, S., Rein, I. D., Stokke, C., Lyng, H., De Angelis, P. M., and Stokke, T. (2011) Three independent mechanisms for arrest in $G_2$ after ionizing radiation. *Cell Cycle* **10,** 819–829

70. Okamoto, K., and Prives, C. (1999) A role of cyclin G in the process of apoptosis. *Oncogene* **18,** 4606–4615

71. Ohtsuka, T., Jensen, M. R., Kim, H. G., Kim, K. T., and Lee, S. W. (2004) The negative role of cyclin G in ATM-dependent p53 activation. *Oncogene* **23,** 5405–5408

72. Seo, H. R., Lee, D. H., Lee, H. J., Baek, M., Bae, S., Soh, J. W., Lee, S. J., Kim, J., and Lee, Y. S. (2006) Cyclin G1 overcomes radiation-induced $G_2$ arrest and increases cell death through transcriptional activation of cyclin B1. *Cell Death Differ* **13,** 1475–1484

73. Bugler, B., Quaranta, M., Aressy, B., Brezak, M. C., Prevost, G., and Ducommun, B. (2006) Genotoxic-activated $G_2$-M checkpoint exit is dependent on CDC25B phosphatase expression. *Mol. Cancer Ther.* **5,** 1446–1451

74. Aressy, B., Bugler, B., Valette, A., Biard, D., and Ducommun, B. (2008) Moderate variations in CDC25B protein levels modulate the response to DNA damaging agents. *Cell Cycle* **7,** 2234–2240

75. Harper, J. W., Adami, G. R., Wei, N., Keyomarsi, K., and Elledge, S. J. (1993) The p21 Cdk-interacting protein Cip1 is a potent inhibitor of G1 cyclin-dependent kinases. *Cell* **75,** 805–816

76. Waldman, T., Kinzler, K. W., and Vogelstein, B. (1995) p21 is necessary for the p53-mediated $G_1$ arrest in human cancer cells. *Cancer Res.* **55,** 5187–5190

77. Bunz, F., Dutriaux, A., Lengauer, C., Waldman, T., Zhou, S., Brown, J. P., Sedivy, J. M., Kinzler, K. W., and Vogelstein, B. (1998) Requirement for p53 and p21 to sustain G2 arrest after DNA damage. *Science* **282,** 1497–1501

78. Lee, J., Kim, J. A., Barbier, V., Fotedar, A., and Fotedar, R. (2009) DNA damage triggers p21WAF1-dependent Emi1 down-regulation that maintains $G_2$ arrest. *Mol. Biol. Cell* **20,** 1891–1902

79. Cazzalini, O., Scovassi, A. I., Savio, M., Stivala, L. A., and Prosperi, E. (2010) Multiple roles of the cell cycle inhibitor p21(CDKN1A) in the DNA damage response. *Mutat. Res.* **704,** 12–20

80. Shimada, M., Nakadai, T., and Tamura, T. A. (2003) TATA-binding protein-like protein (TLP/TRF2/TLF) negatively regulates cell cycle progression and is required for the stress-mediated $G_2$ checkpoint. *Mol. Cell. Biol.* **23,** 4107–4120

81. Suenaga, Y., Ozaki, T., Tanaka, Y., Bu, Y., Kamijo, T., Tokuhisa, T., Nakagawara, A., and Tamura, T. A. (2009) TATA-binding protein (TBP)-like protein is engaged in etoposide-induced apoptosis through

transcriptional activation of human TAp63 gene. *J. Biol. Chem.* **284,** 35433–35440

82. Welcsh, P. L., Lee, M. K., Gonzalez-Hernandez, R. M., Black, D. J., Mahadevappa, M., Swisher, E. M., Warrington, J. A., and King, M. C. (2002) BRCA1 transcriptionally regulates genes involved in breast tumorigenesis. *Proc. Natl. Acad. Sci. U.S.A.* **99,** 7560–7565

83. Bae, I., Fan, S., Meng, Q., Rih, J. K., Kim, H. J., Kang, H. J., Xu, J., Goldberg, I. D., Jaiswal, A. K., and Rosen, E. M. (2004) BRCA1 induces antioxidant gene expression and resistance to oxidative stress. *Cancer Res.* **64,** 7893–7909

84. Merbl, Y., and Kirschner, M. W. (2009) Large scale detection of ubiquitination substrates using cell extracts and protein microarrays. *Proc. Natl. Acad. Sci. U.S.A.* **106,** 2543–2548

85. Faradji, F., Bloyer, S., Dardalhon-Cuménal, D., Randsholt, N. B., and Peronnet, F. (2011) *Drosophila melanogaster* cyclin G coordinates cell growth and cell proliferation. *Cell Cycle* **10,** 805–818